Printed to pdf: August 12, 2010

MFT-Radfys 2010:01

department of Radiation physics, GU

Monte Carlo simulation of treatment machine Varian Clinac iX

Emma Hedin

University of Gothenburg

Roumiana Chakarova, Anna Bäck, Janos Swanpalmer

MSF Sahlgrenska University Hospital

Abstract

This report presents methods and results from the development of a Monte Carlo model of a Varian Clinac iX linear accelerator of nominal energy 6 MV. The simulations are made by the BEAMnrc/EGSnrc Monte Carlo code package [1]. The model is adjusted for open fields. Wedge fields can be simulated by step-and-shoot method. In a future work, the model will be further developed by including MLC component.

This report describes in detail how model parameters are optimised and how the quality of the model is verified. The parameters adjusted in the model are the energy of the electrons (monoenergetic) incident (normally) on the target as well as the width of the spatial distribution of the electrons (assumed to be Gaussian). The accelerator head is simulated in one step and the dose distribution in water is calculated in a subsequent step. Simulated data are compared to measured data visually, quantatively by directly comparing the numbers and by statistically weighting the differences in a chi^2/NDF analysis.

The optimum parameter set is found to be 5.7 MeV and 0.1 cm (FWHM). The agreement between measured and simulated data is found to be good. The measured and simulated data agreed to within 1% except in the case of depth dose for a 2x2 cm^2 field and for profiles at dose maximum.

Contents

1 Introduction

Dose calculation algorithms used in treatment planning systems (TPS) are approximations of the real particle interactions in the human tissue. The generic opinion is that Monte Carlo calculations of radiation environments yields the most correct dose distributions available and Monte Carlo calculations are used as reference when evaluation of different approximations is made. This report focuses on the development of a Monte Carlo model of a linear accelerator used in the clinic to treat patients with radiation therapy.

A model of a Varian Clinac iX machine at the radiation treatment department at Sahlgrenska University Hospital (room 8) was built in BEAMnrc (a Monte Carlo code dedicated to radiation therapy) according to technical data provided by Varian. The technical data given was specified being intended to be used in the context of doing Monte Carlo simulations. It should be noted that several densities were not specified and dimensions presented were not always consistent.

Generally when building a Monte Carlo model, simulated data is compared to measured data. The radiation fields are characterised by profiles at different depths, depth dose curves and output factors. The Monte Carlo model is described by a number of free parameters apart from those determined in technical documentation. Typically, the properties of the bremsstrahlung generating electron beam are parameters allowed to vary in the work of adjusting the model to measured data. In the literature one can find investigations of for instance beam width, mean energy and energy spread. Finding estimates of the free parameters is a trial and error strategy. A certain parameter set is assigned and the dose distribution is simulated and compared to the measured dose in order to determine weather the parameter set is good enough. If not, the parameters are adjusted and the simulation is repeated until the measured-simulated consistency is good enough according to some preset conditions.

Several authors have investigated how the parameters in the model affects the simulated profiles, depth dose curve and output factor of a photon field. For example Sheikh-Bagheri & Rogers [2] give a detailed analysis of the effect of factors such as properties of the electron beam, properties of the flattening filter, lateral dimensions of the target etc. They state that the simulated depth dose curve is not sensitive to the width of the electron beam and they also present a method of comparing measured and simulated profiles in air. In order to adjust the simulated data to be in accordance with measured data their conclusion is that angle, energy distribution and divergence of the electron beam are in practice best held constant. This leaves mean energyand the width of the electron beam to be varied. This strategy is used in the method presented by Khaled *et.al.* [3]. J Pena *et.al.* [4] show that the profile of large fields is sensitive both to energy and width of the electron beam and state that electron beam

parameters can be found by only comparing profiles (and not depth dose curves) from large fields to measured data. They also claim better energy resolution using this method since depth dose curves are only sensitive to energy changes of size 0.3 MeV. P. J. Keall *et. al.* [5] analyse three parameters to describe their Monte Carlo accelerator model, namely; electron energy, width of the electron beam and the target density. Sham *et. al.* (2008) [6] recently introduced the concept of adjusting focal spot width by comparing measured and simulated data for small fields, i.e. fields in the order of 0.5x0.5 cm^2.

Other authors having published results from building accelerator models of comparable Varian machine-types in BEAMnrc is; Sheikh-Bagheri & Rogers [2] who present model parameters of mean energy 5.7 MeV and focal spot width 0.1 cm for a Clinac high energy machine using 3% energy spread and P. J. Keall [5] who present model parameters of mean energy 6.2 MeV and 0.13 cm focal spot width (FWHM) for a 2100 EX Varian machine, also using 3% energy spread. B. Ask [7] presents a table of some more references and the work of adjusting modeling parameters for a Varian Clinac-23EX machine which resulted in the parameters: energy 6.4 MeV (monoenergetic) and 0.12 cm focal spot witdh. This gives the reader an idea of the nature of the work of developing a Monte Carlo model of a linear accelerator. Even though one models two machines of the same type the measured data sets will differ and the parameters adjusted in the Monte Carlo model will be different.

2 Material/methods

A model of the linear accelerator Varian Clinac iX was defined in BEAMnrc (Graphical User Interface 2.0) based on technical data provided by Varian Medical Systems. Densities and dimensions were kept constant during the simulations. The calculations were made partly on a local computer with an Intel Core-2 Duo processor (1066MHz FSB, 4MB L2) using Ubuntu operating system and partly on a Linux cluster on the National Supercomputer Centre (NSC), Linköping, Sweden (operating system CentOS 5 x86_64 and Intel Xeon E5345 processors). On NSC the program was run in a parallell mode, using several processors for each job. Parameters for the virtual model were derived for a 6 MV nominal energy photon beam.

The accelerator head was simulated in one step and the dose distribution in water was calculated in a subsequent step. The radiation field was stored in an intermediate phase-space file containing information about the particle speed, direction and charge/type. The phase space file was also used for simulation of an in-air dose profiles, a method described in section 2.6.1. The iterative method of optimising the model is described schematically in Figure 1.

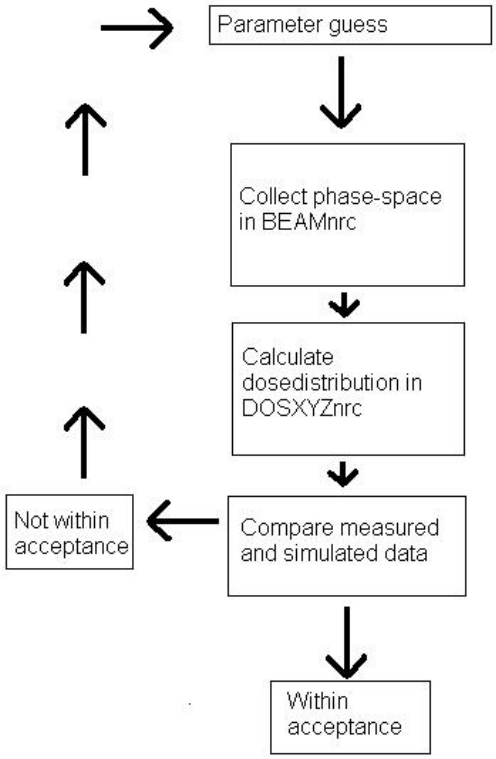

Figure 1: Schematic sketch describing the iterativ method of finding the optimum parameter set describing the radiation field.

2.1 Accelerator head simulation in BEAMnrc

A parallel circular beam of electrons hitting the target with gaussian radial distribution (BEAMnrc: source number 19) was used to simulate the electron ray in the production of the phase-space files. The electron beam was assumed to be monoenergetic. The parameters, electron energy and width of the electron beam hitting the target, were varied to fit the model to the measured data. The width of the gaussian radial distribution, the focal spot width (FSW), was defined as the Full Width at Half Maximum (FWHM) of the distribution (i.e the width of the distribution where the distribution is half of its maximum value). The electron beam was set to be incident normal to the target surface. A sketch over the accelerator head and schematic boxes symbolizing phase space and the region with dose distribution of interest are shown in Figure 2.

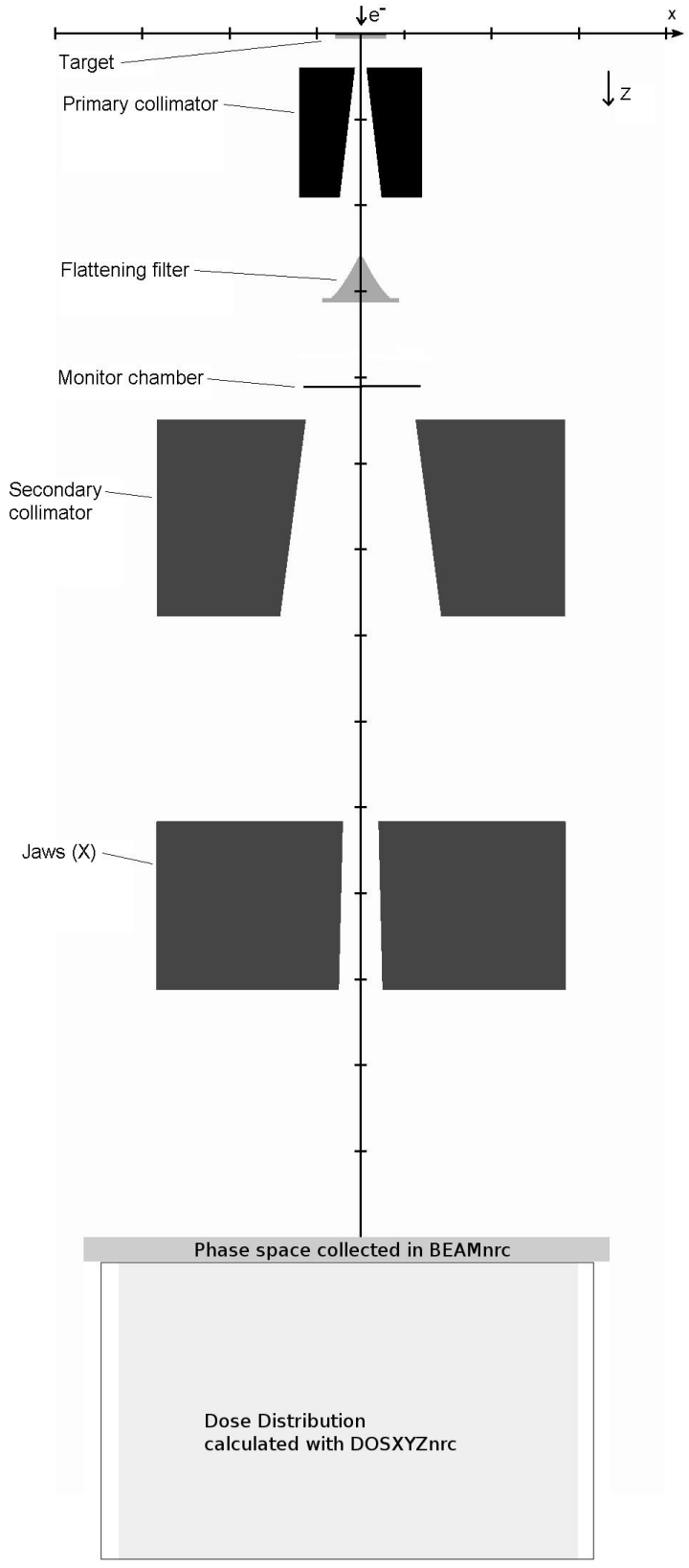

Figure 2: Schematic sketch over the accelerator head, phase space collection and region with dose distribution of interest. x/z-plot at y=0 (central axis). Y direction Jaws not visible in this plane when separated.

The global photon and electron cut-off energy was 0.01 MeV and 0.7 MeV respectively. The variance reduction technique of directional bremsstrahlung (DBS) was used. The splitting number was set to 1000 and the electron splitting was performed in the lower layers of the flattening filter as recommended in the BEAMnrc users manual [1]. Range rejection was turned on with varying ECUTRR (= the minimum energy a charged particle needs to be able to reach the bottom of the accelerator and still having more than 0.7 MeV). Range rejection was considered for electrons with energy less than 2 MeV (ESAVE_GLOBAL = 2) except for in the target where range rejection was considered for electrons with energies less than 1 MeV. The same range rejection run parameters have for example been used by Hasenbalg *et. al.* [8].

Simulations were made for several combinations of electron energy and FSW. For each parameter combination the dose distribution of several different field sizes were analysed. The parameters were varied until a parameter combination was satisfactory as described in Figure 1. The optimum parameter combination was then verified by simulating the field sizes presented in Table 2.

2.2 Simulation of profiles in-air with BEAMDP

A first estimate of the energy of the electrons incident on the target was found by comparing collision kerma profiles collected in air for different energies with measured profiles, as described by Sheikh-Bagheri *et. al.* [2]. Water-kerma-profiles (collision) were produced by processing the phase-space file in a modified version of BEAMDP. The weight of each photon is multiplied by its energy, mass-energy-absorption coefficient (Hubbel and Seltzer [9]) and one over the cosine of the angle its direction makes with the z-axis. Only the photons from the phase-space-file were taken into account, the contamination electrons were not included as they are assumed to not influence the measurement. The collision kerma profiles were normalised to the value at the central axis. This ratio will in the remainder of this report be referred to as the off-axis factor. The collision kerma was assumed to be proportional to the signal from an ionisation chamber. An assumption based on the principles of small detector cavities in which the photons are very unlikely to contribute directly to ionisation but more likely via electrons.

The BEAMDP-method is fast since the step of calculating dose distribution in the DOSXYZnrc is avoided. The energy found by this method is regarded to be a first coarse estimate because only one distance from the target, namely the distance at which the phase-space is collected, is considered. Also, a change in FSW may influence the optimum energy. However, as stated in the results, the optimum energy found from the in-air simulations is not sensitive to changes in FSW below 0.1 cm. The insensitivity of the optimum energy to FSW-changes in the in-air

simulations is extensively analysed by Sheikh-Bagheri & Rogers [2].

2.3 Calculation of dose distributions in water

The dose profiles in water phantom were calculated using the Monte Carlo code DOSXYZnrc. The depth dose-curves were calculated with the CHAMBER module in BEAMnrc. No range rejection was used. The electrons were tracked until their energy was below 0.512 MeV and the photons were tracked until their energy was below 0.010 MeV. The edge of the phantom was kept more than 10 cm away from the field edge and more than 10 cm deeper than the last data point.

In DOSXYZnrc the region of interest was divided into voxels with dimensions depending on the resolution selected. When simulating dose profiles for fields larger than 4x4 cm^2 the central voxels were 1 cm wide (square top area) and the remaining voxels were 0.3 cm wide. In the cases of 4x4 cm^2 and 2x2 cm^2 field sizes the central voxels were 0.5 cm wide and the remaining were 0.5 cm and 0.2 cm wide, respectively. The voxel widths in the case of 4x4 cm^2 and 2x2 cm^2 field sizes were chosen to correspond to the dimensions of the ionisation chambers to make the simulated penumbral region comparable to the measured. Because of the measurement uncertainties associated with the size of the detector and its material the smallest field size considered in this work was 2x2 cm^2. The depth dose (BEAMnrc) values were determined in 0.2 cm high standing cylinders with a radius of 0.75 cm at the central axis, except for the case of 2x2 cm^2 field size. In this case the cylinders were 0.3 cm high with a radius of 0.15 cm.

In the stage of doing simulations for several different parameter combinations (see Section 2.6), dose profiles were extracted at 1.5, 5 and 10 cm depth with the voxels 0.5 cm deep. When the optimum parameter set was found, dose profiles were recalculated at 1.5, 5, 10 and 20 cm depth using voxels 0.5, 0.5, 0.5 and 1 cm deep, respectively. The measured dose profiles for 40x40 cm^2 field size were half-profiles. The simulated profiles were in this case averaged over positive and negative x-axis to receive better statistics.

2.4 Ionisation chamber measurements

The in-air measurements were performed at a distance of 100 cm from the top of the target using a cylindrical ionisation chamber (Exradin T2 Spokas Thimble chamber, 0.53 cm^3) with a build-up cap of brass. The centre of the chamber was used as reference point when positioning the chamber (SSD 100 cm). The chamber was used in conjunction with a 3 mm thick brass build-up cap to ensure charged particle equilibrium over the measuring cavity. In this situation the chamber signal was assumed to be proportional to dose to water in the centre of the

chamber. The chamber was moved across the field in the x-axis direction (defined by the lower jaws) with 1.5 cm step size, starting at the central axis. The value at the central axis was measured at the start of the measurement and then repeated after the first half of the profile measurement was completed. No chamber correction was made for changes in temperature and pressure. A complete profile measurement took between 30 minutes and one hour. No corrections were made for change in chamber response due to beam-quality changes over the profile.

The water measurements were performed using ionisation chambers. For field sizes larger than 2x2 cm^2 the compact chamber CC13, manufactured by Iba Dosimetry was used (0.13 cm^3, inner air cavity diameter 0.6 cm). For field size 2x2 cm^2 the PTW Pin-Point (0.015 cm^3, inner cavity diameter 0.2 cm, central electrode of steel) chamber was utilized. The SSD was equal to 100 cm in all water phantom measurements except for the case of the assymetric 10x10 cm^2 field. The dose profile for this assymetric field was measured using the compact chamber CC04 (0.04 cm^3, inner cavity diameter 0.4 cm) at a distance of 90 cm from the top surface of the target.

2.5 Comparison, measurement-simulation

The measured and simulated dose profiles and depth dose curves were compared visually and in some cases also by two different cost functions, namely chi^2/NDF and the number of simulated data points deviating more than a given percentage from the measured profile. The value of chi^2/NDF was calculated according to Equation 1.

$$\chi^2/NDF = \sum_{i=1}^{N} \frac{(s_i - m_i)^2}{\sigma_i^2}/(N-1), \tag{1}$$

where m_i and s_i are the measured and simulated normalised dose values, respectively. σ_i is the standard error of the $i:th$ simulated value and N is the number of data points compared. NDF (Number of Degrees of Freedom) is in this case $N-1$ since σ is estimated using s_i (for more details regarding the statistics, see the BEAMnrc users manual [1] or B. R. B. Walters *et. al.* [10]).

The build-up region is not considered to be accurately simulated and measured depth dose data is only compared to simulated data beyond dose maximum. A comparison between simulations in the build-up region is presented in the appendix along with a discussion regarding differences in simulation methods and versions of BEAMnrc.

2.6 Finding the optimum parameter combination

2.6.1 In-air simulations

The field sizes and parameter combinations used for in-air simulations are presented in Table 1.

Table 1: Table presenting the field sizes and parameter combinations used for in-air simulations. x = simulation has been made. Columns 3-9 represent different energies (MeV).

field size (cm^2)	**FSW (cm)**	**5.2**	**5.4**	**5.5**	**5.6**	**5.7**	**5.8**	**6.0**
40x40	0.05						x	
40x40	0.1						x	
30x30	0.05			x	x		x	x
20x20	0.05	x	x		x	x	x	

2.6.2 Dose profiles

Preparatory simulations were made for a 10x10 cm^2 field when keeping the energy at a value of 6 MeV and varying the FSW from 1 cm to 0.06 cm. As stated in the results this preparatory study indicated that no change can be observed below 0.1 cm for such a small field (10x10 cm^2), larger field sizes must be considered. Profile-simulations in order to find the optimum set of parameters were made for 20x20 and 40x40 cm^2 field sizes. Field size 40x40 cm^2 was simulated for the following parameter combinations; 5.8 MeV with 0.05 and 0.1 cm FSW as well as 5.7 Mev with 0.08, 0.1 and 0.15 cm FSW. Field size 20x20 cm^2 was simulated for the same parameter combinations except for the parameter combination 5.7 MeV and 0.08 cm FSW. The parameter combination start values were based partly on previous studies on similar machines and on the results from in-air simulations which, as given in the results, suggested an energy of approximately 5.7 MeV. At this stage of optimising the parameters, dose profiles in x-direction (defined by the lower pair of collimators) were analysed.

2.6.3 Depth Dose

Preparatory simulations were made for a 10x10 cm^2 field keeping the FSW at a value of 0.06 cm and varying the energy in steps of 0.2 MeV from 5.2 MeV to 6.4 MeV. This gave an indication of the responsiveness of the depth dose curve to energy changes.

2.7 Verifying the optimum parameter combination

The optimum parameter combination was verified through simulation of the fields listed in Table 2. When verifying the model for the field sizes 10x10 and 20x20 cm^2 y-direction (defined by the upper pair of collimators) dose profiles were included in the analysis.

Table 2: Table presenting the field sizes simulated in BEAMnrc when verifying the optimum parameter combination. In the second column the associated DBS-radius defined at a distance 100 cm from the top of the target is given. In the last column the calculated dose distributions are given.

field size (cm^2)	**DBS-radius** (cm)	
2x2	10	Depth dose, Profile
4x4	20	Depth dose, Profile
10x10	20	Depth dose, Profile
20x20	30	Depth dose, Profile
40x40	30	Depth dose, Profile
10x10*	20,30	Profile
x4y20**	???	Profile

*Assymetric, see expl. below

**Retangle, see expl. below

When verifying the optimum parameter set a 10x10 cm^2 assymetric field was simulated with assymetric position of the field edges in x-direction. The central axis coincided with the field edge (Doselevel 50% of maximum???, SSD=100 cm). The simulation of assymetric fields is essential for treatment plans containing joint fields. A symmetric (around the central axis) but rectangularly shaped field with dimensions x=4 cm and y=20 cm was also simulated to further test the performance of the model.

Once the optimum parameter combination had been obtained, output factors were calculated for the symmetrical fields in Table 2. The output factors were defined as the ratio between the dose at the central axis at 10 cm depth, for a given field size, and the dose at central axis at 10 cm depth for the 10x10 cm^2 square reference field. The dose at 10 cm depth was assessed in two different ways; from (i) a fifth grade polynomial fitted to dose values between depth 5 cm and 20 cm and (ii) from the voxel containing the point of interest.

3 Results

The statistical uncertainties of the in-air simulations were low. The phase-space-files consisted of around 3.5E8 particles for 20x20 cm^2 field size and between 2E8 and 8E8 particles for 30x30 cm^2 field size (no recycling). The relative uncertainty (1 standard deviation) of the simulated values were 0.1% or smaller. The statistical uncertainties of the in-water simulations varied. However, when the optimum parameter set had been found and the work of verifying the chosen parameter set (Section 3.2) started, we found that the in-water dose distribution calculations required more than $1 * 10^7$ histories run per square centimeter field size (at SSD equal to 100 cm) to receive desireable statistical uncertainties. The particles were recycled 10 to 15 times.

3.1 Finding the optimum parameter set

3.1.1 In-air

Changing the value of FSW from 0.1 to 0.05 cm did not significantly influence the in-air profiles. The simulated off-axis factors for different energies, keeping FSW at 0.05 cm, are presented in the diagrams in Figure 3 together with the measured off-axis-factors. The off-axis distances were 12 cm and 7.5 cm for 30x30 and 20x20 cm^2 field size, respectively. The off-axis distance was chosen to avoid dose gradients. The optimum energy for 0.05 cm FSW was found to be 5.71 and 5.78 MeV for 20x20 and 30x30 cm^2 field size, respectively. The error in the determined energy because of uncertainty in the simulated off-axis-factors was hard to determine from the residuals of the linear fit (too few degrees of freedom yielded ± 0.5 MeV 95% confidence interval of the energy from LINEST (excel 2003) and the t-distribution). In an attempt to take into account the uncertainty of the simulated off-axis-factors a linear fit was made for maximum simulated off-axis factors (profile value +95% confidence interval) and for the minimum simulated off-axis factor (profile value -95% confidence interval) respectively. The difference in energy was 0.06MeV. Assuming the error of the measured off-axis factor to be ± 0.25% the uncertainty of the determined energy propagates to be ± 0.07 MeV. The energy intervals should not be considered as statistical confidence intervals and are to be added to yield the precision of the method. This makes the method precise to ± 0.1 MeV at best.

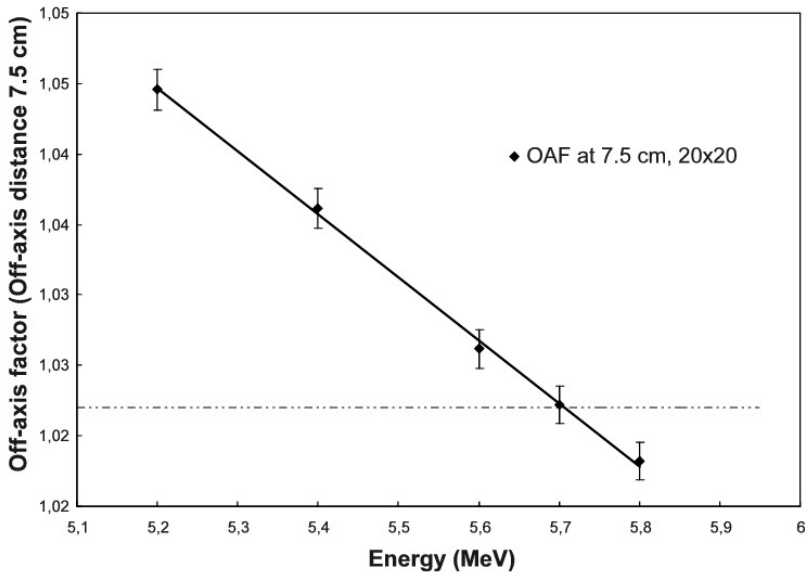

(a)

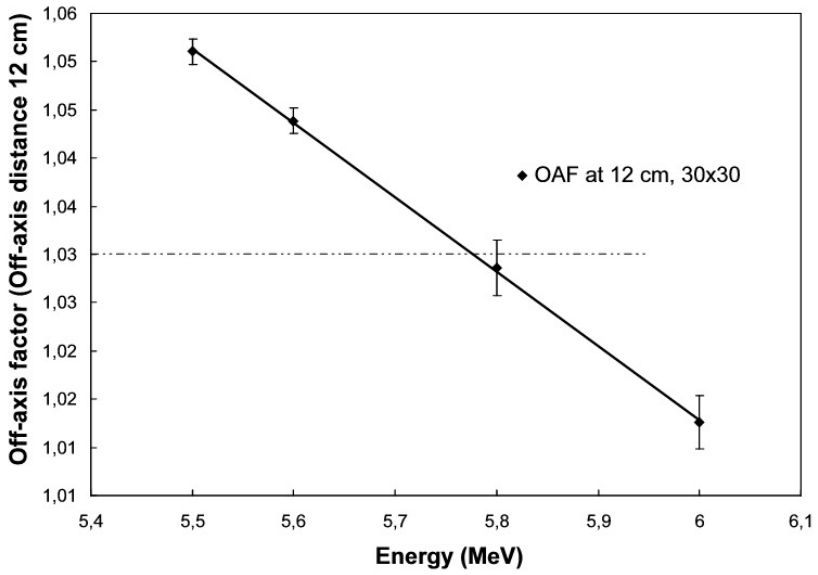

(b)

Figure 3: Off-axis factors (OAF) plotted against the energy of electrons incident on the target for the field sizes (a) 20x20 cm^2 and (b) 30x30 cm^2. The dashed line represents the measured value of off-axis factor at 7.5 cm and 12 cm off axis distance, respectively. The errorbars represent the 95% confidence interval of the simulated data points.

3.1.2 Profiles

The preparatory simulations suggested no change in lateral profiles when going below 0.1 cm FSW for a 10x10 cm^2 field. Moreover it showed that the energy guess of 5.7 MeV yielded optimised profiles in combination with FSW 0.1 cm that were in very good compliance with measured data. The profiles for the optimum parameter set is shown in section 3.2.1.

3.1.3 Depth dose

Regarding depth dose curves, energies between 5.6 and 6.2 MeV could be considered equally good when compromising between good fit at dose-max and good fit at deeper depths (discarding any change in depth dose curve due to FSW). However as shown in Figure 4 (125 degrees of freedom, depth 3 to 30 cm), the chi^2 analysis was clearly pointing to an optimum energy of 6 MeV when 0.06 cm FSW was used.

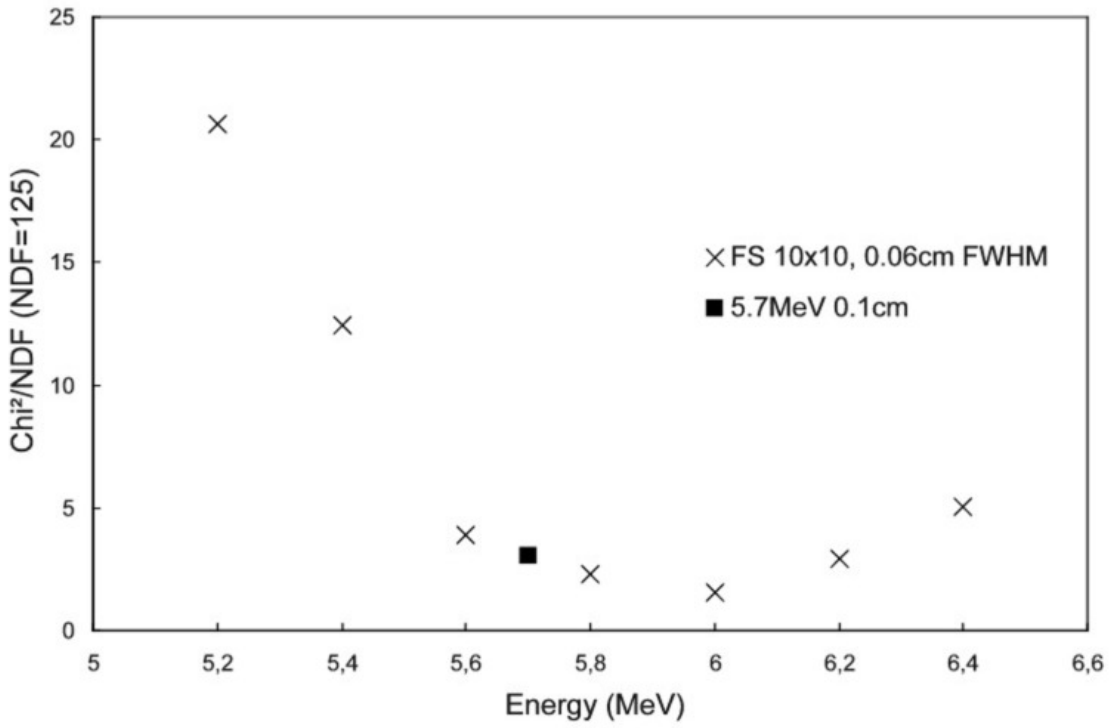

Figure 4: chi^2/NDF for depth dose curves from a 10x10 cm^2 field plotted against energy of the on the target incident electrons. Focal spot width kept constant at 0.05 cm, energy varied from 5.2 to 6.4 MeV. Errobars ($2 * \sqrt{2/NDF}$) represented by the size of the data points. NDF=125, depths between 3 and 30 cm.

3.2 Verifying the optimum parameter set

3.2.1 Dose Profiles

The optimum parameter set was chosen to be; 5.7 MeV energy of the electrons incident on the target and 0.1 cm FSW. Corresponding profiles are shown in Figures 5 to 9. All profiles go through the central axis. The dose has been normalised to the dose at central axis for each depth.

The simulated and measured profiles for 40x40 cm^2 field size for parameter set [5.7 MeV 0.1 cm] are seen in Figure 5. None of the simulated data points, between x=0 and x=19.75 cm, in Figure 5 a), b), c) and d) deviate from measured data more than 1.5%, 1%, 1% and 1.8% of the central axis dose at the given depth, respectively. The deviation should be considered in conjunction with the relative standard errors of the normalised simulated values which, within the actual interval, are between 0.3% and 0.4%.

The simulated and measured profiles for 20x20 cm^2 field size for parameter set [5.7 MeV 0.1 cm], are seen in Figure 6. None of the simulated data points between, x=-8.95 and x=8.95 cm in Figure 6 a), b), c) and d) deviate from measured data more than 1.4%, 1%, 1.3% and 1.2% of the central axis dose at the given depth, respectively. The deviation should be considered together with the relative standard errors of the normalised simulated values which, within the actual interval, are between 0.45% and 0.55%.

The chosen parameter set [5.7 MeV 0.1 cm] was further verified for field sizes 10x10, 4x4 and 2x2 cm^2. These profiles are shown in Figures 7 to 9. In the case of 10x10 cm^2 field size none of the simulated data points between x=-4.25 and x=4.25 cm in Figure 7 a), b), c) and d) deviate from measured data more than 1.7%, 1%, 1.5% and 1.2% of the central axis dose at the given depth, respectively. The deviation should be considered in conjunction with the relative standard errors of the normalised simulated values which, within the actual interval, are around 0.4%.

The field sizes 4x4 and 2x2cm^2 were analysed visually and the simulated penumbra was assured to agree with measured data to within 1 mm except for at 1.5 cm depth for the 2x2 cm^2 field and both 1.5 cm and 5 cm depth for the 4x4 cm^2 field, where the difference was between 1 and 1.5 mm. This larger difference was observed at only one of the field edges. It should be noted that the measured fields are not centered.

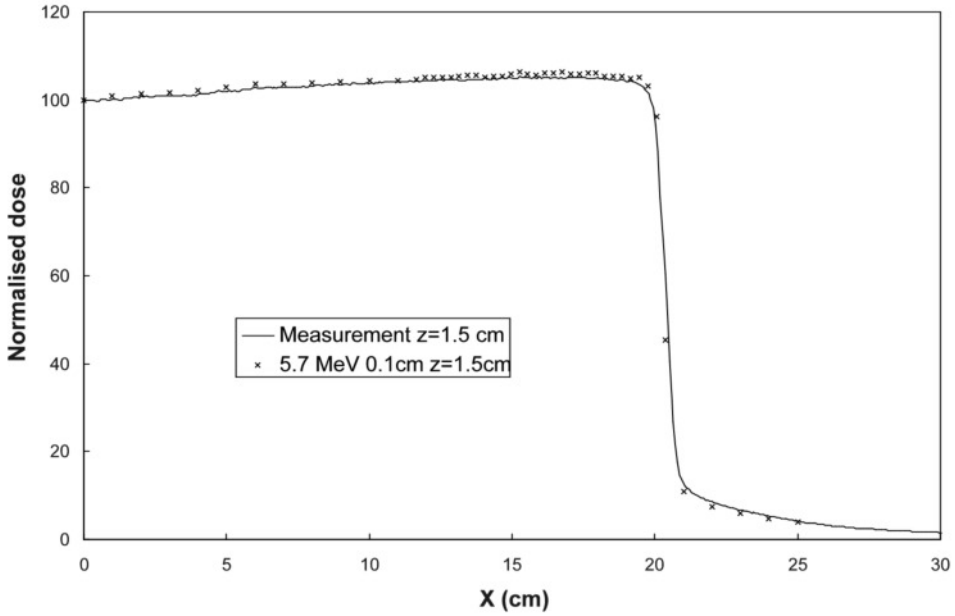
Normalised dose
X (cm)
Measurement z=1.5 cm
5.7 MeV 0.1cm z=1.5cm
0
20
40
60
80
100
120
0
5
10
15
20
25
30

(a)

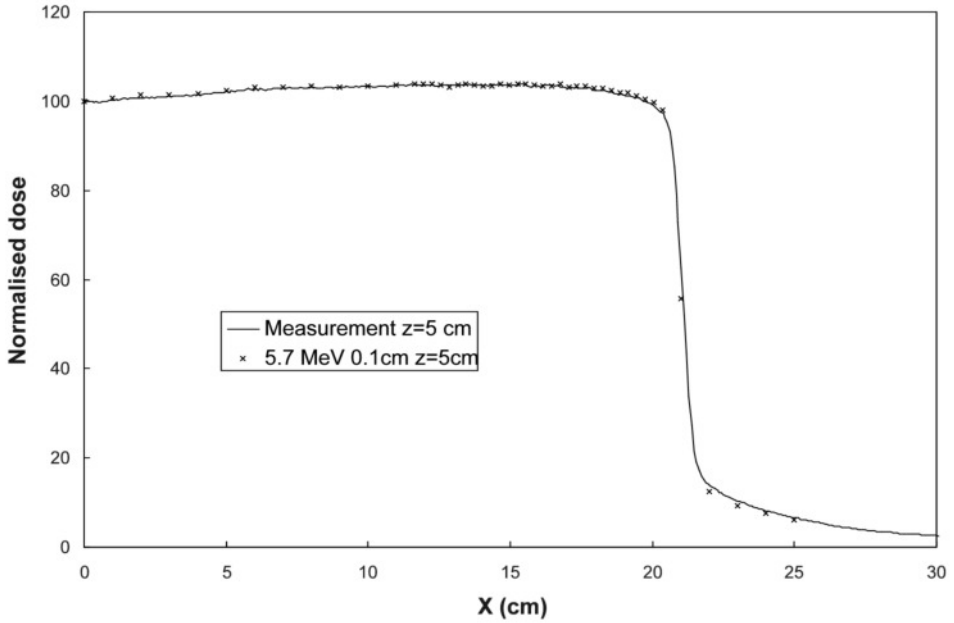
Normalised dose
X (cm)
Measurement z=5 cm
5.7 MeV 0.1cm z=5cm
0
20
40
60
80
100
120
0
5
10
15
20
25
30

(b)

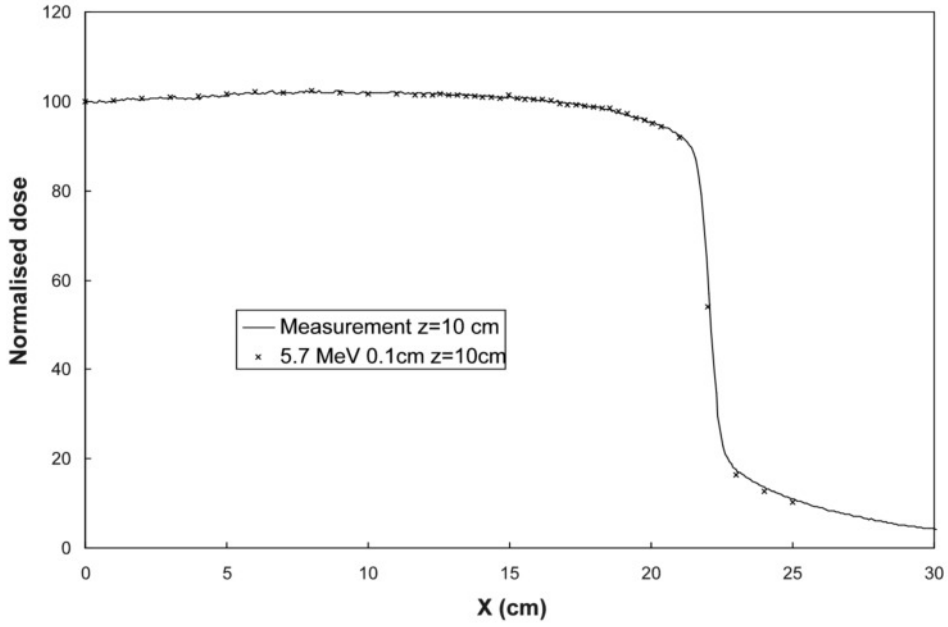

(c)

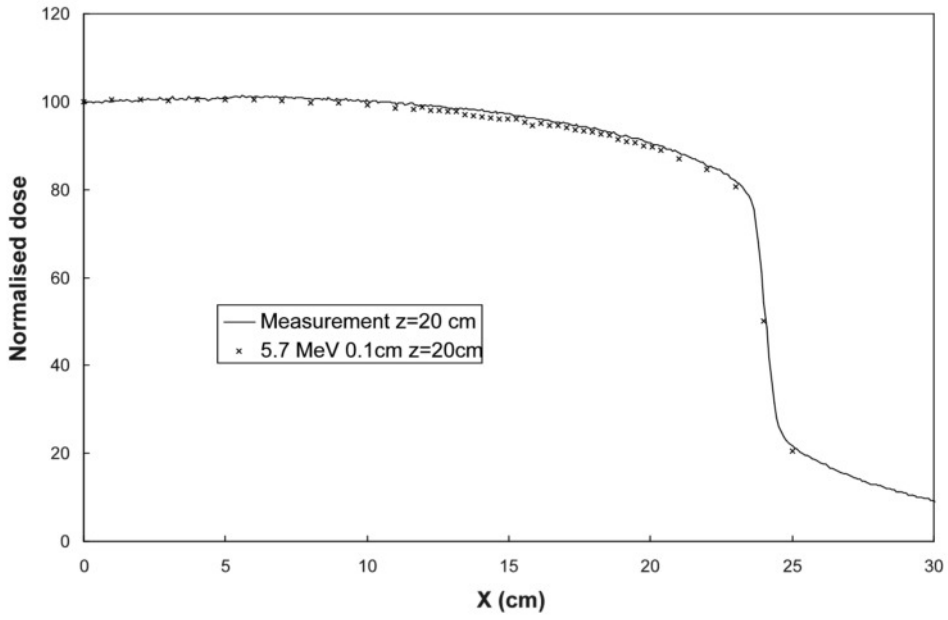

(d)

Figure 5: Dose profile for 40x40 cm^2 field size in water phantom at a) 1.5 cm, b) 5 cm, c) 10 cm, d) 20 cm depth. Solid line measured (CC13) and discrete points simulated. The uncertainties of the simulated values (+-1SE) are represented by the size of the data points. Deviation between measured and simulated data is less than a) 1.5%, b) 1%, c) 1%, d) 1.8% of the dose at central axis in the range x=0 to 19.75 *cm*.

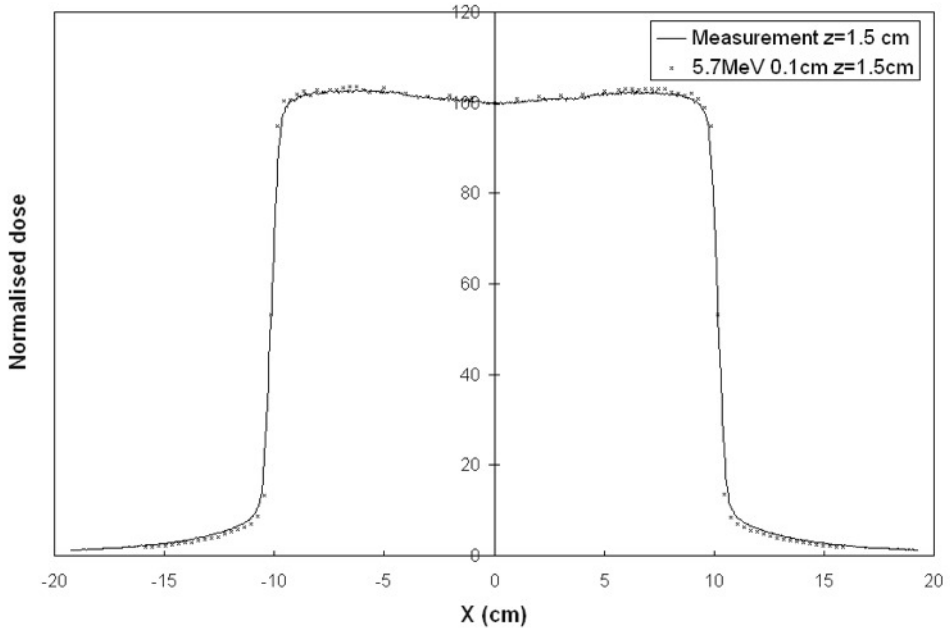
Measurement z=1.5 cm
5.7MeV 0.1cm z=1.5cm
Normalised dose
X (cm)
120
100
80
60
40
20
0
-20
-15
-10
-5
0
5
10
15
20

(a)

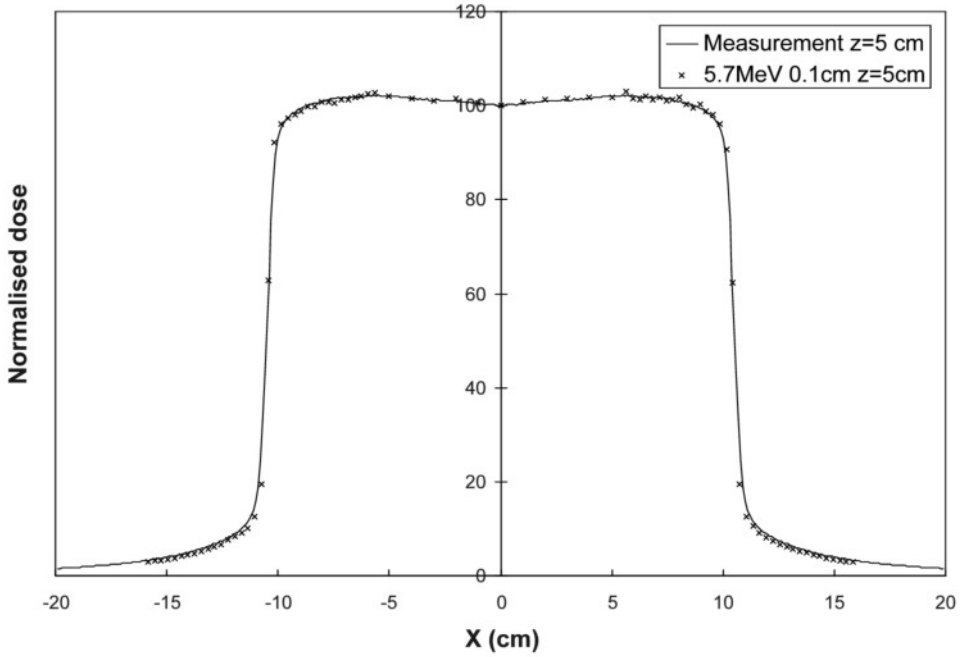
Measurement z=5 cm
5.7MeV 0.1cm z=5cm
Normalised dose
X (cm)
120
100
80
60
40
20
0
-20
-15
-10
-5
0
5
10
15
20

(b)

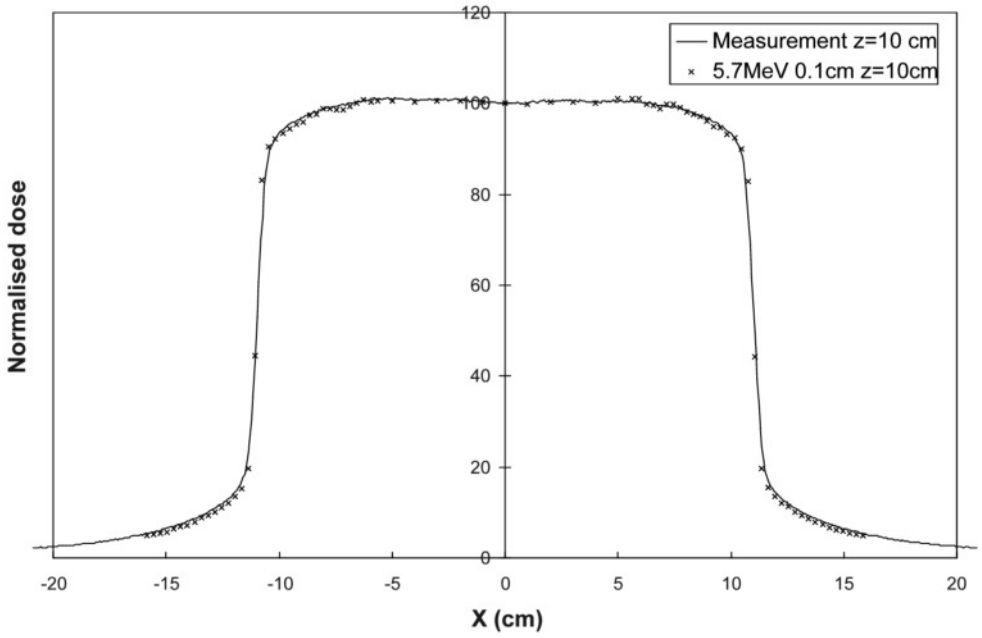

(c)

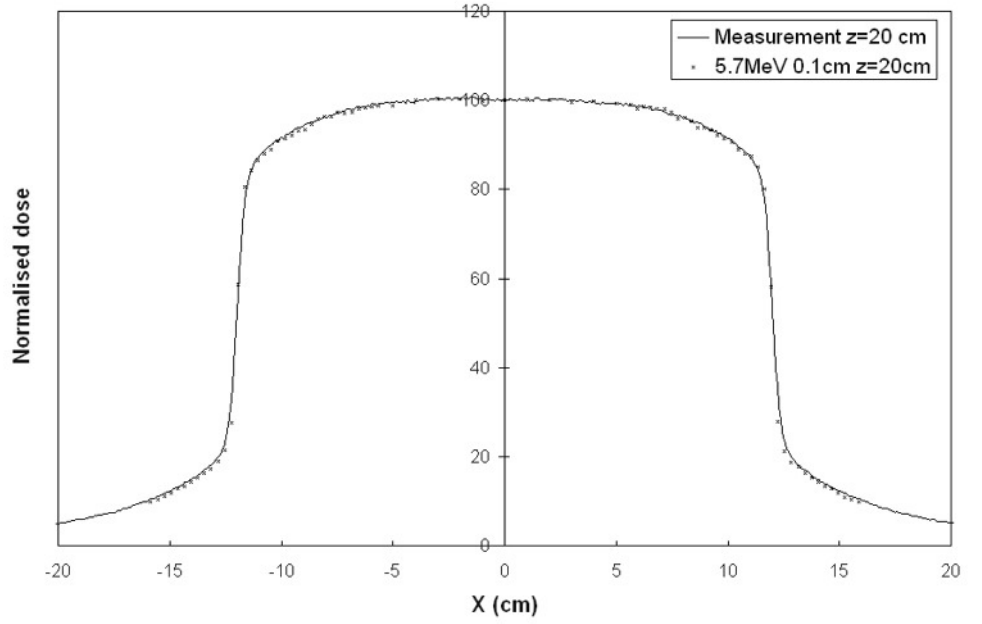

(d)

Figure 6: Dose profile for 20x20 cm^2 field size in water phantom at a) 1.5 cm, b) 5 cm, c) 10 cm, d) 20 cm depth. Solid line measured (CC13) and discrete points simulated. The uncertainties of the simulated values (+-1SE) are represented by the size of the data points. Deviation between measured and simulated data is less than a) 1.4%, b) 1%, c) 1.3%, d) 1.2% of the dose at central axis in the range x=-8.95 to x=8.95 *cm*.

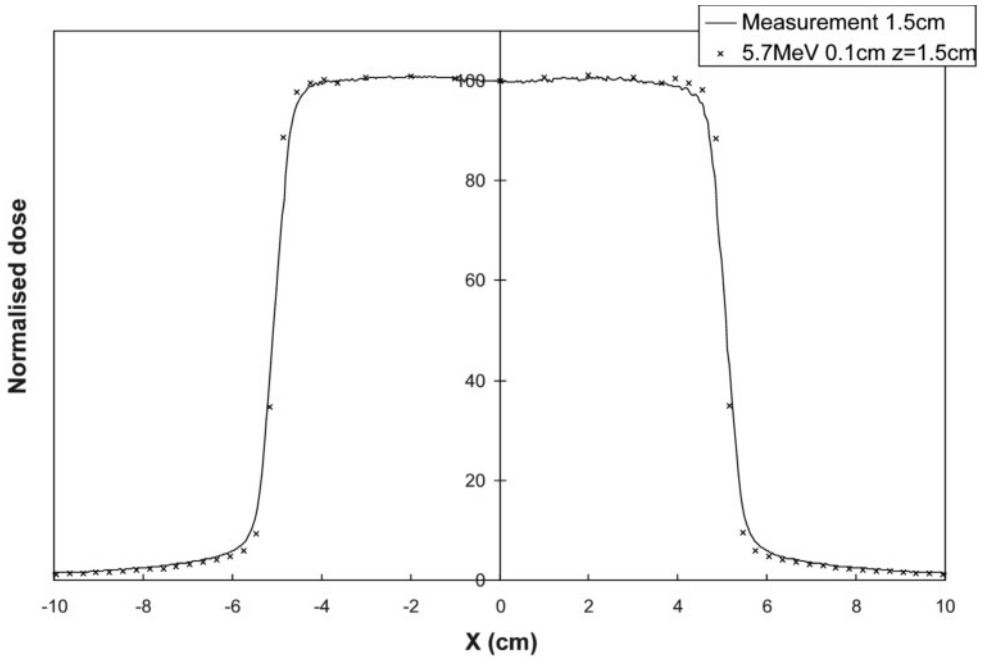
Measurement 1.5cm
5.7MeV 0.1cm z=1.5cm
Normalised dose
X (cm)
0
20
40
60
80
100
-10
-8
-6
-4
-2
0
2
4
6
8
10

(a)

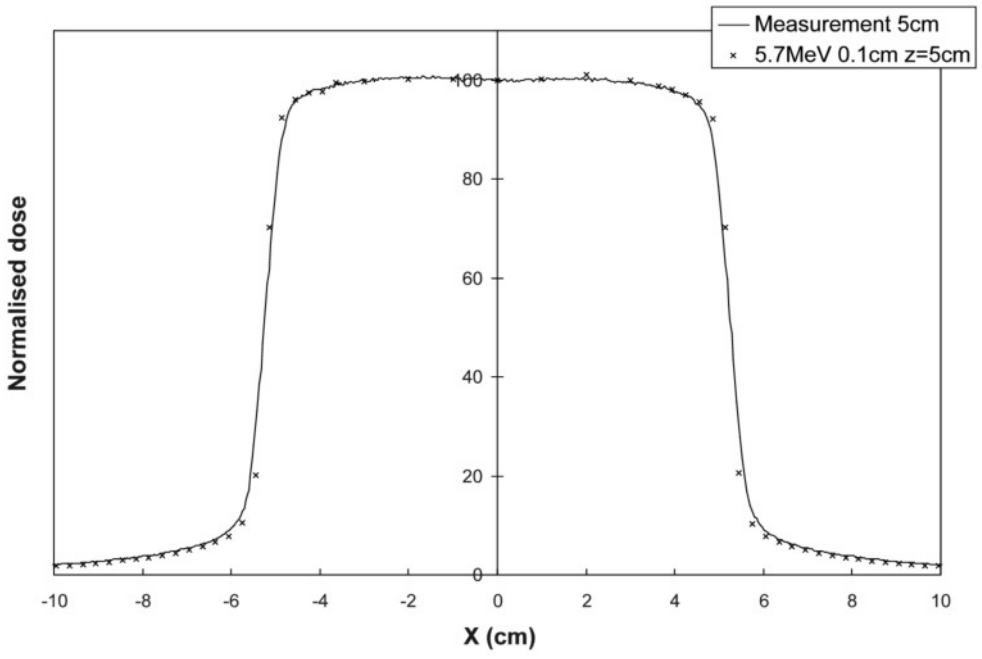
Measurement 5cm
5.7MeV 0.1cm z=5cm
Normalised dose
X (cm)
0
20
40
60
80
100
-10
-8
-6
-4
-2
0
2
4
6
8
10

(b)

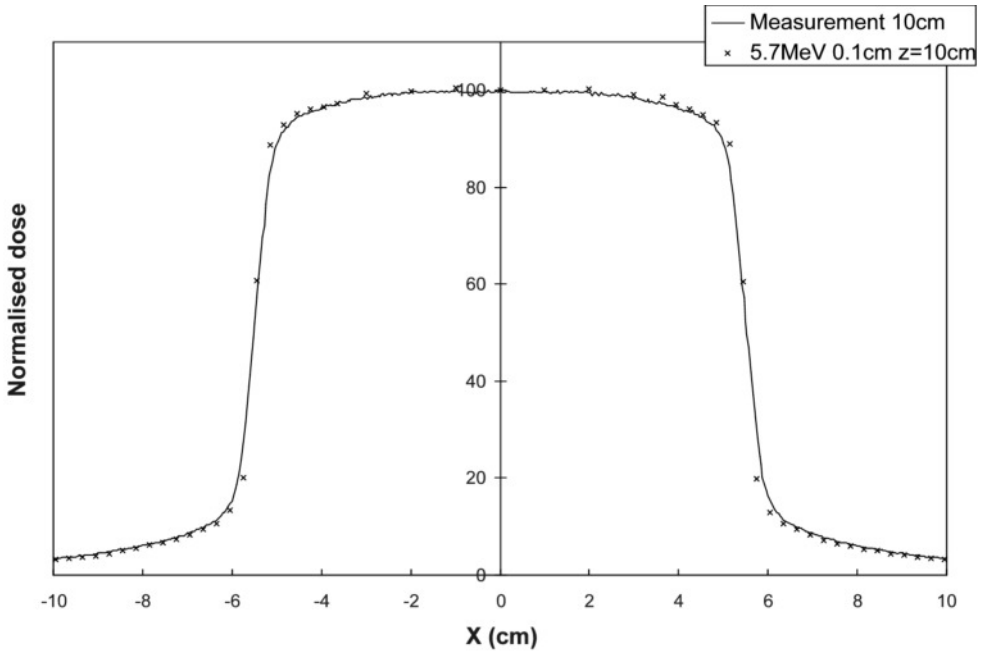

(c)

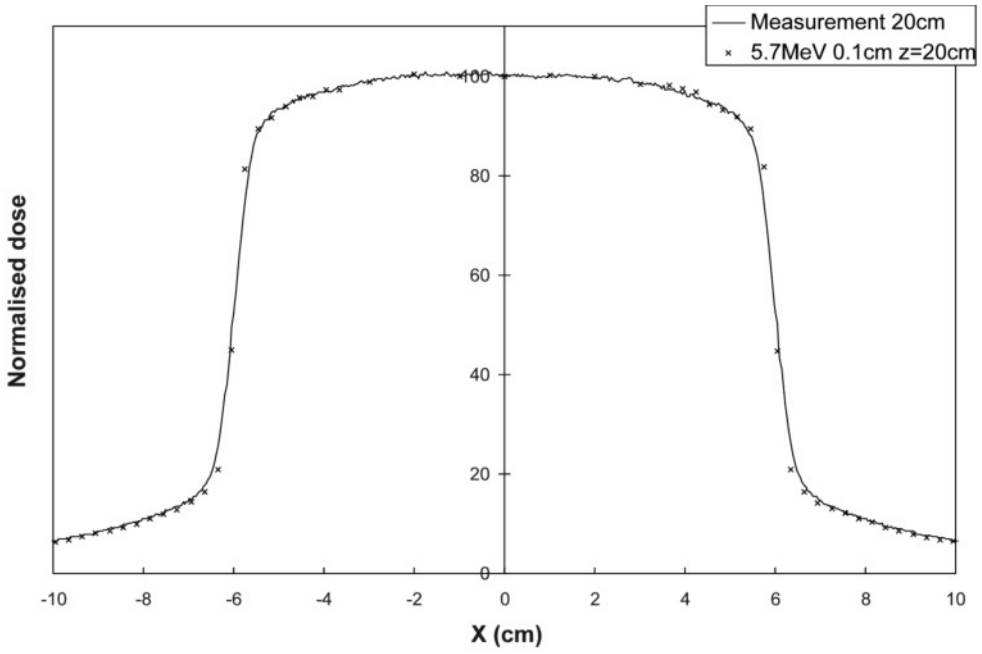

(d)

Figure 7: Dose profile for 10x10 cm^2 field size in water phantom at a) 1.5 cm, b) 5 cm, c) 10 cm, d) 20 cm depth. Solid line measured (CC13) and discrete points simulated. The uncertainties of the simulated values (+-1SE) are represented by the size of the data points. Deviation between measured and simulated data is less than a) 1.7%, b) 1%, c) 1.5%, d) 1.2% of the dose at central axis in the range x=-4.25 to x=4.25 *cm*.

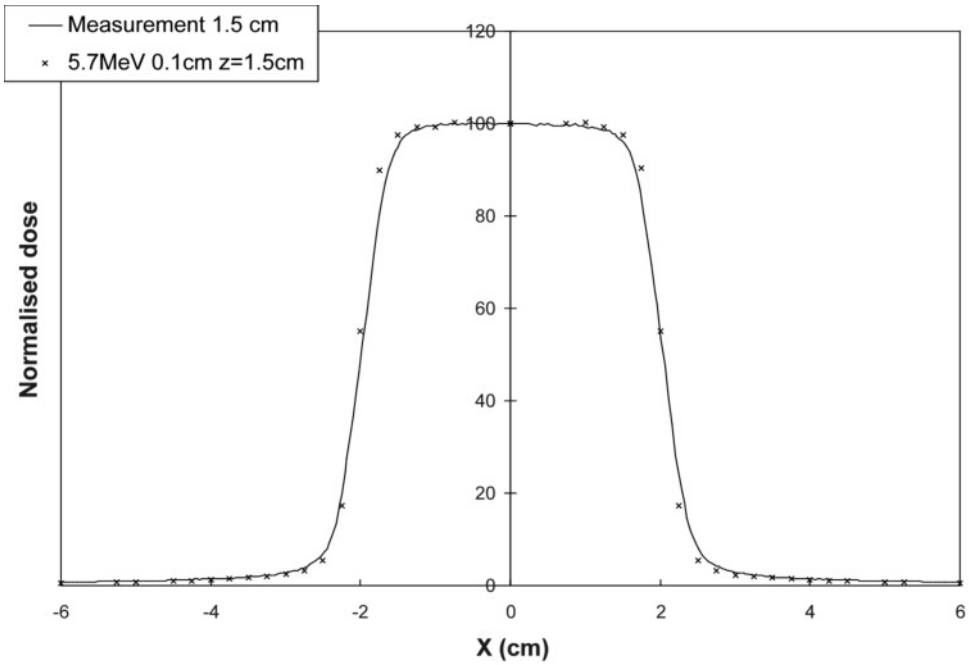
Measurement 1.5 cm
5.7MeV 0.1cm z=1.5cm
Normalised dose
X (cm)
120
100
80
60
40
20
0
-6
-4
-2
0
2
4
6

(a)

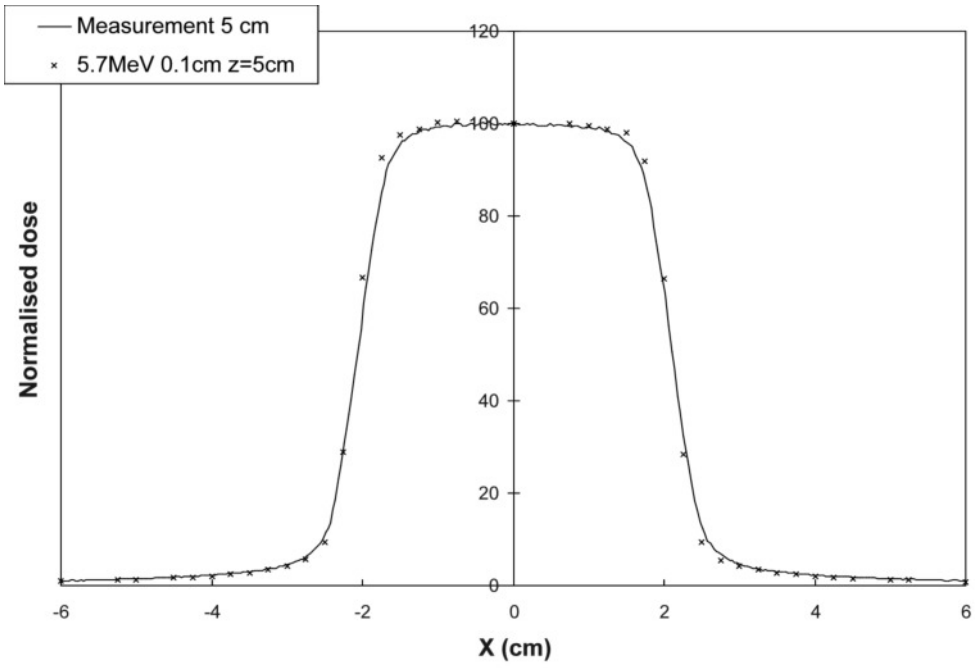
Measurement 5 cm
5.7MeV 0.1cm z=5cm
Normalised dose
X (cm)
120
100
80
60
40
20
0
-6
-4
-2
0
2
4
6

(b)

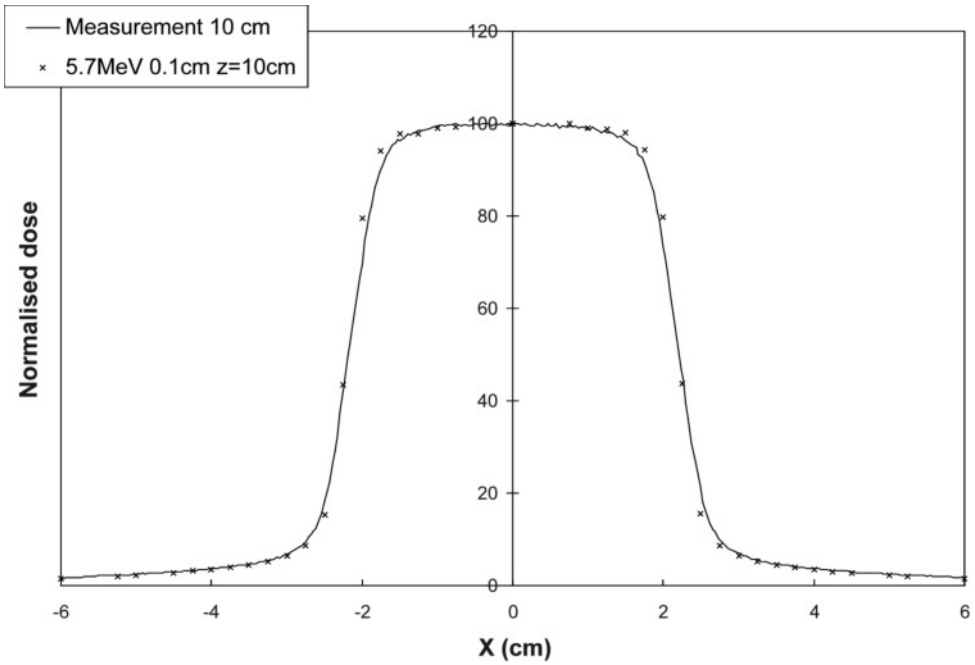

(c)

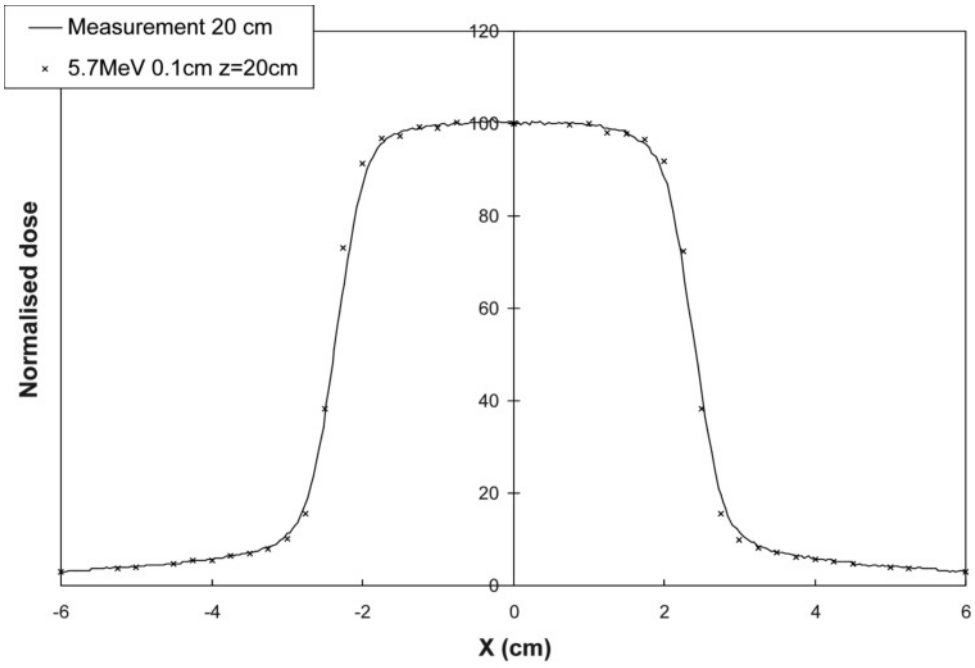

(d)

Figure 8: Dose profile for 4x4 cm^2 field size in water phantom at a) 1.5 cm, b) 5 cm, c) 10 cm, d) 20 cm depth. Solid line measured (CC13) and discrete points simulated. The uncertainties of the simulated values (+-1SE) are represented by the size of the data points.

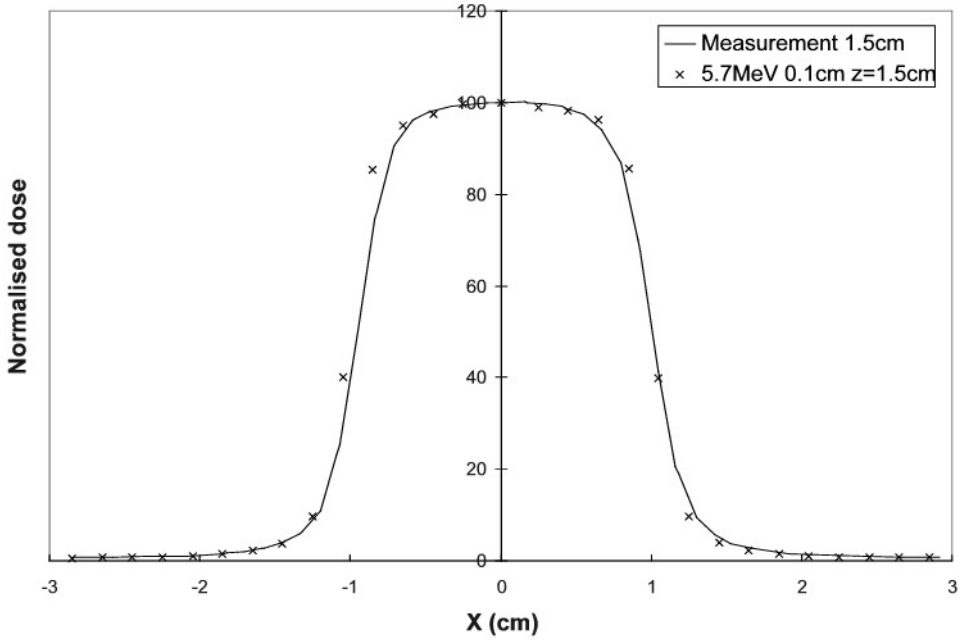
Measurement 1.5cm
5.7MeV 0.1cm z=1.5cm
Normalised dose
X (cm)
120
100
80
60
40
20
0
-3
-2
-1
0
1
2
3

(a)

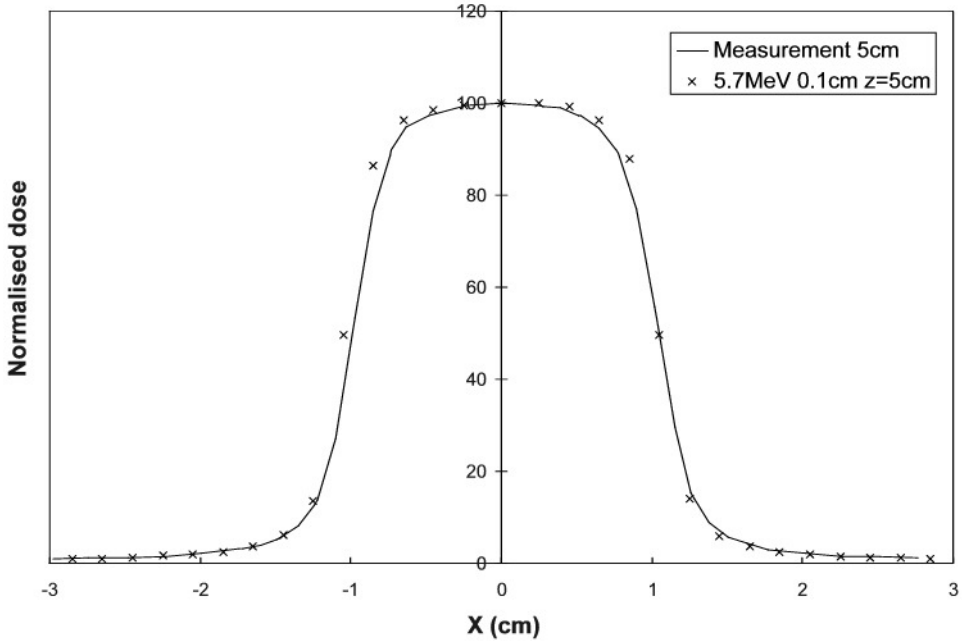
Measurement 5cm
5.7MeV 0.1cm z=5cm
Normalised dose
X (cm)
120
100
80
60
40
20
0
-3
-2
-1
0
1
2
3

(b)

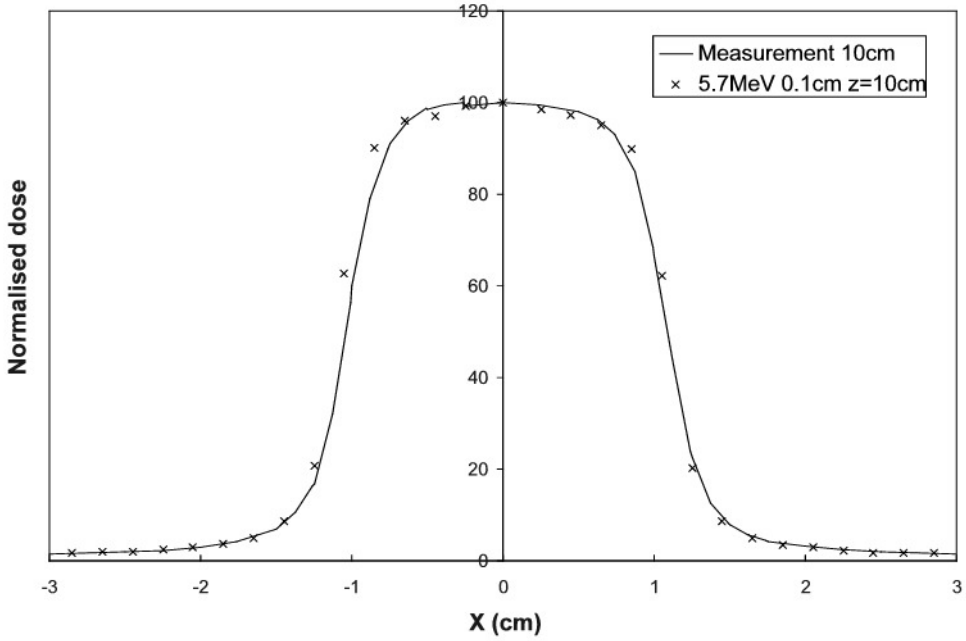

(c)

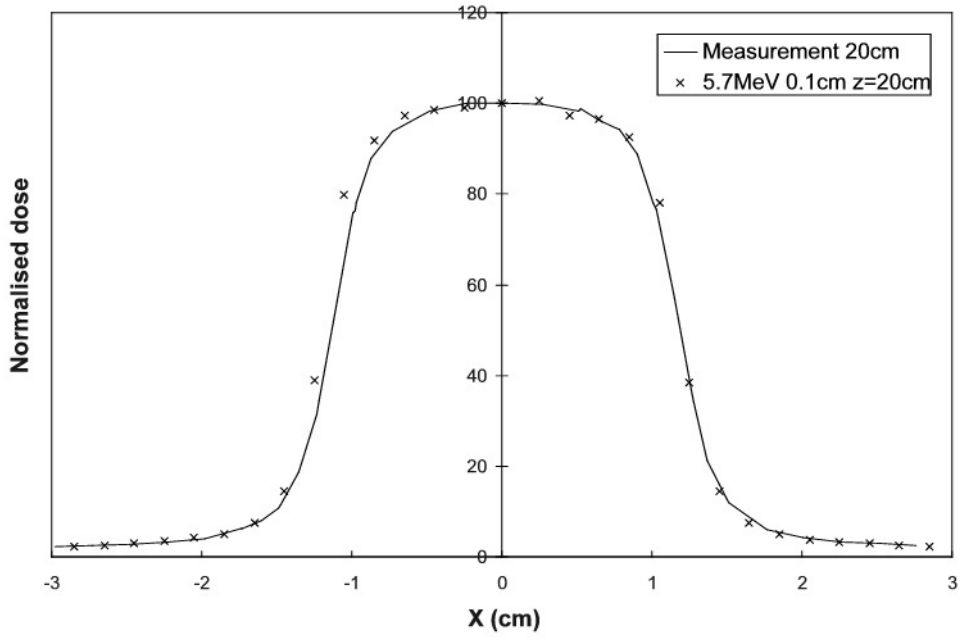

(d)

Figure 9: Dose profile for 2x2 cm^2 field size in water phantom at a) 1.5 cm, b) 5 cm, c) 10 cm, d) 20 cm depth. Solid line measured (pin-point, steel electrode) and discrete points simulated. The uncertainties of the simulated values (+-1SE) are represented by the size of the data points.

3.2.2 Y-direction Dose Profiles

Dose profiles in y-direction were analysed visually for a 10x10 cm^2 and a 20x20 cm^2 field. The comparison between measured and simulated data are shown in Figures 10 to 11.

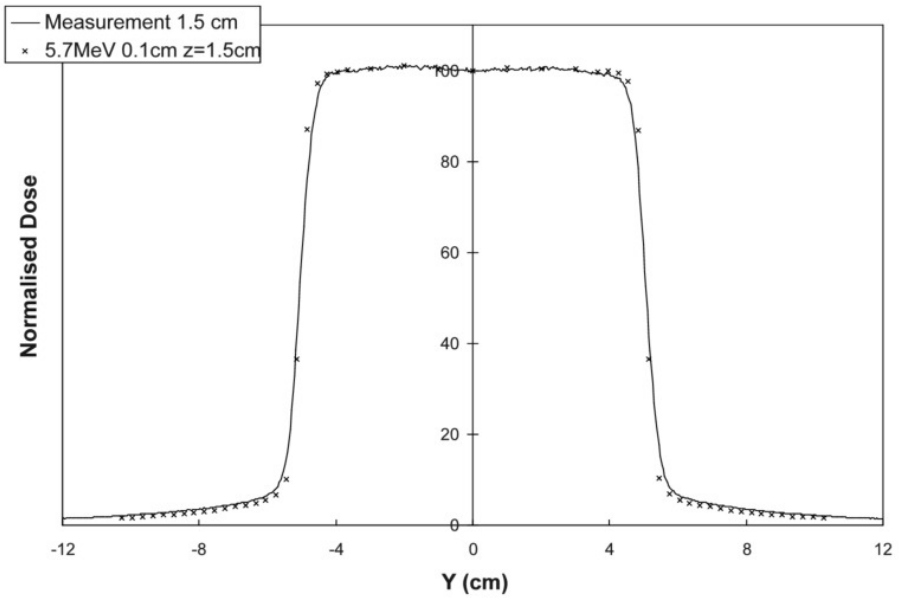

(a)

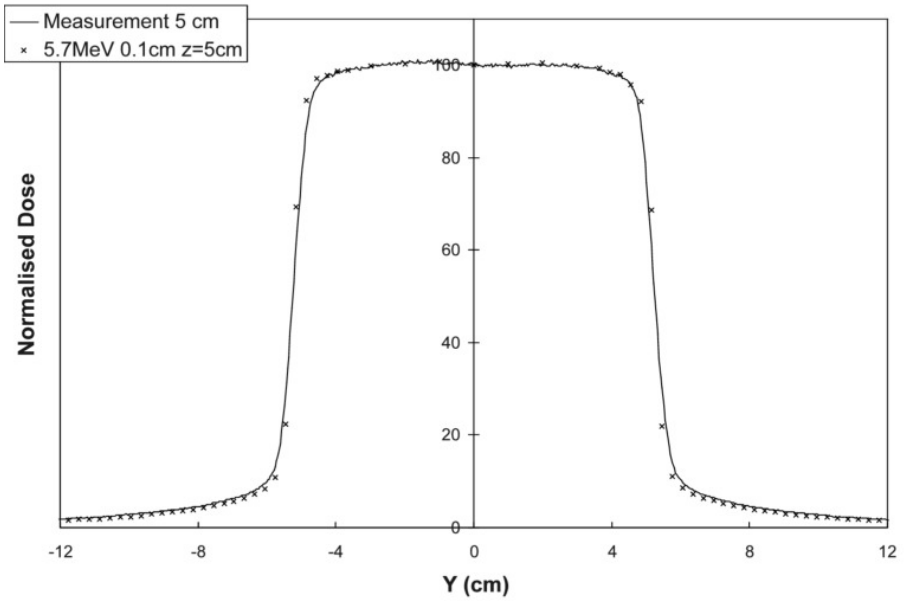

(b)

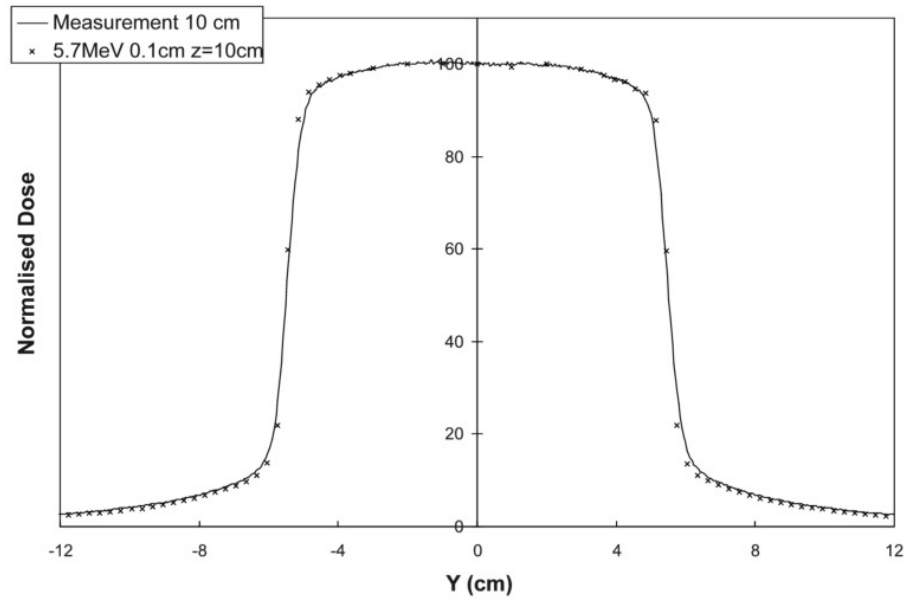

(c)

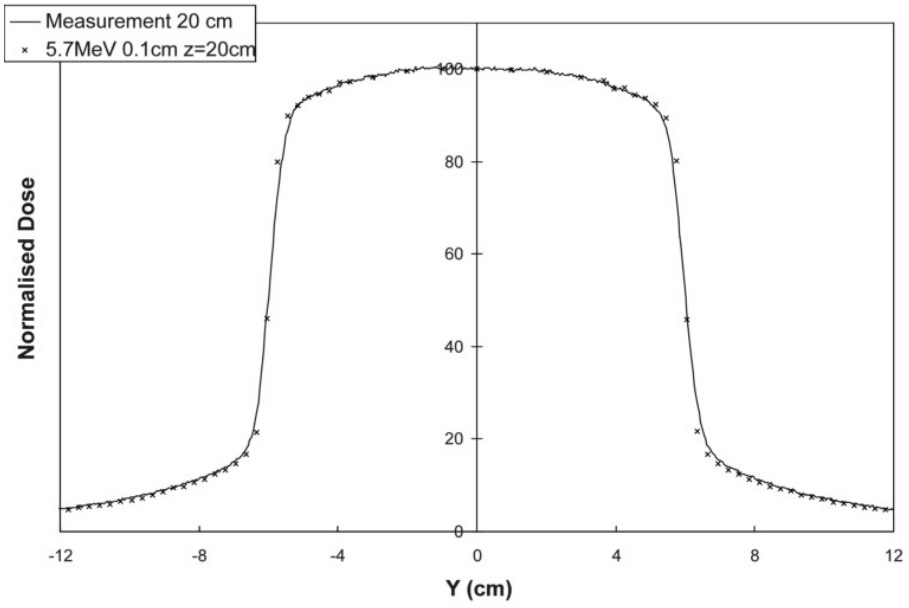

(d)

Figure 10: Y-direction dose profile for 10x10 cm^2 field size in water phantom at a) 1.5 cm, b) 5 cm, c) 10 cm, d) 20 cm depth. Solid line measured (CC13) and discrete points simulated. The uncertainties of the simulated values (+-1SE) are represented by the size of the data points.

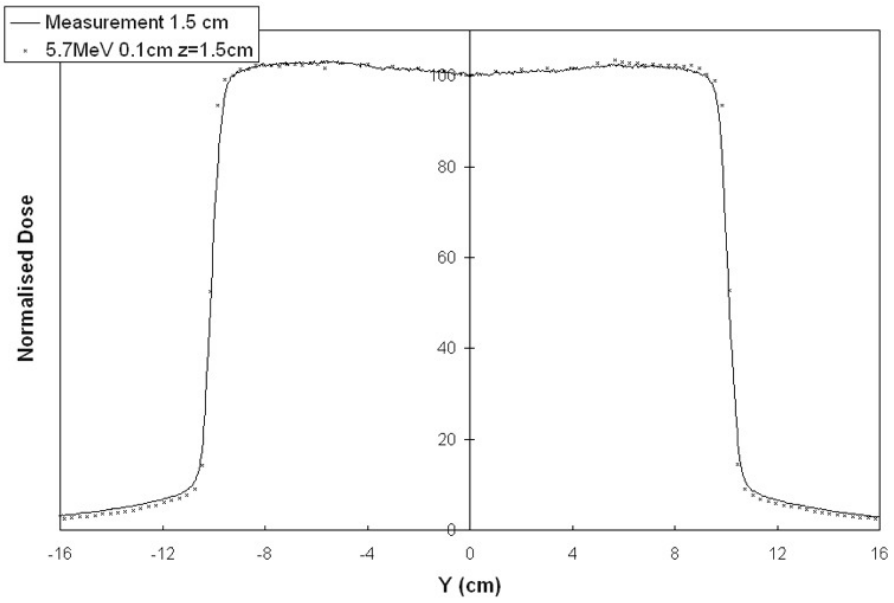
Measurement 1.5 cm
5.7MeV 0.1cm z=1.5cm
Normalised Dose
Y (cm)
0
20
40
60
80
100
-16
-12
-8
-4
0
4
8
12
16

(a)

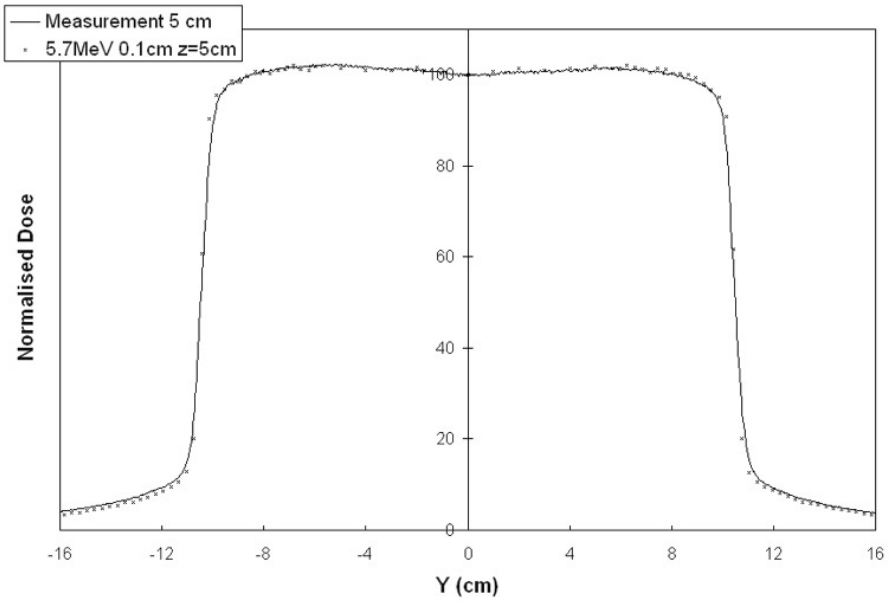
Measurement 5 cm
5.7MeV 0.1cm z=5cm
Normalised Dose
Y (cm)
0
20
40
60
80
100
-16
-12
-8
-4
0
4
8
12
16

(b)

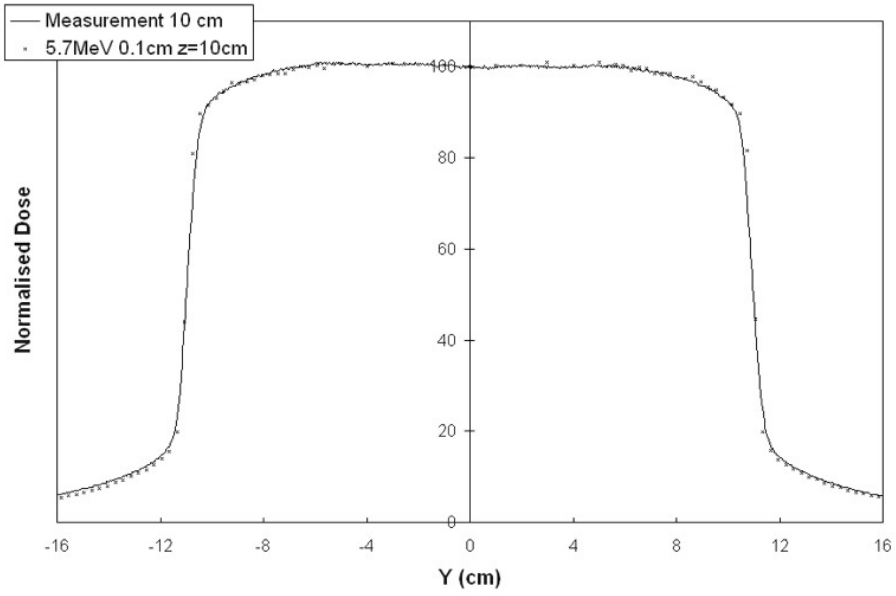

(c)

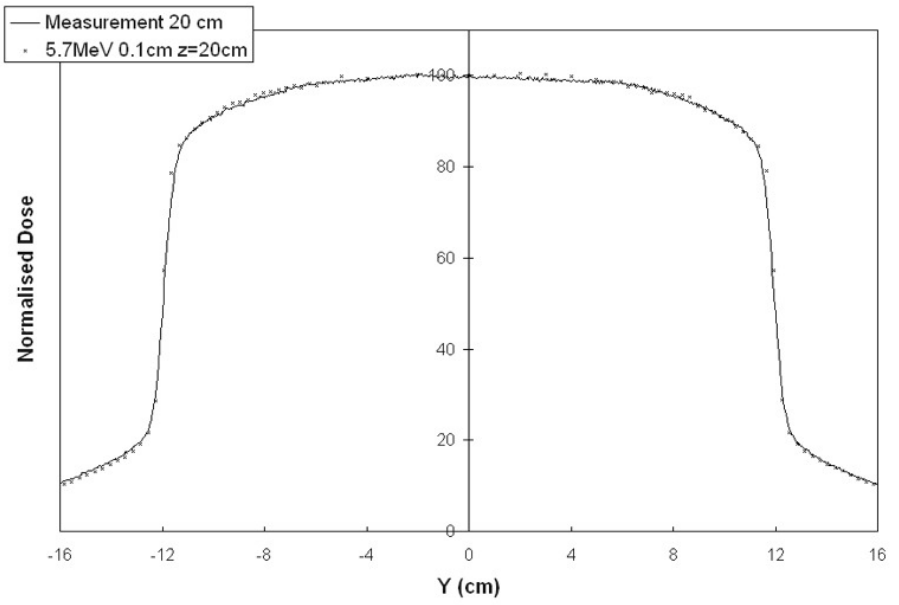

(d)

Figure 11: Y-direction dose profile for 20x20 cm^2 field size in water phantom at a) 1.5 cm, b) 5 cm, c) 10 cm, d) 20 cm depth. Solid line measured (CC13) and discrete points simulated. The uncertainty of the simulated values (+-1SE) are represented by the size of the data points.

3.2.3 Depth Dose Curves

The depth dose verification curves for parameter set [5.7 MeV 0.1 cm] are shown in Figures 12 to 16. The dose has been normalised (100%) to dose at 10 cm depth, taken from a fifth grade polynomial fitted to the simulated data points between the depths 5 and 20 cm. In all cases the simulated data points do not deviate more than 1% (of the dose in dose max) from the measured data between the depth of dose max and 25 cm, except for in the case of the 2x2 cm^2 field, in which the deviation at dose maximum is 2.5% of the dose at dose maximum.

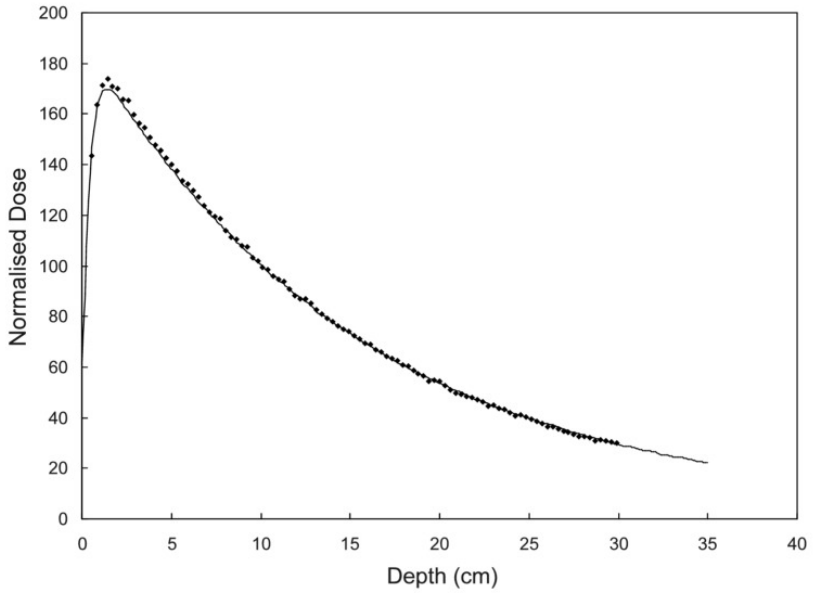

Figure 12: Depth dose curve for 2x2 cm^2 field size in water phantom. Solid line measured (pin-point, steel electrode) and discrete points simulated. The uncertainties of the simulated values (±1SE) are represented by the size of the data points.

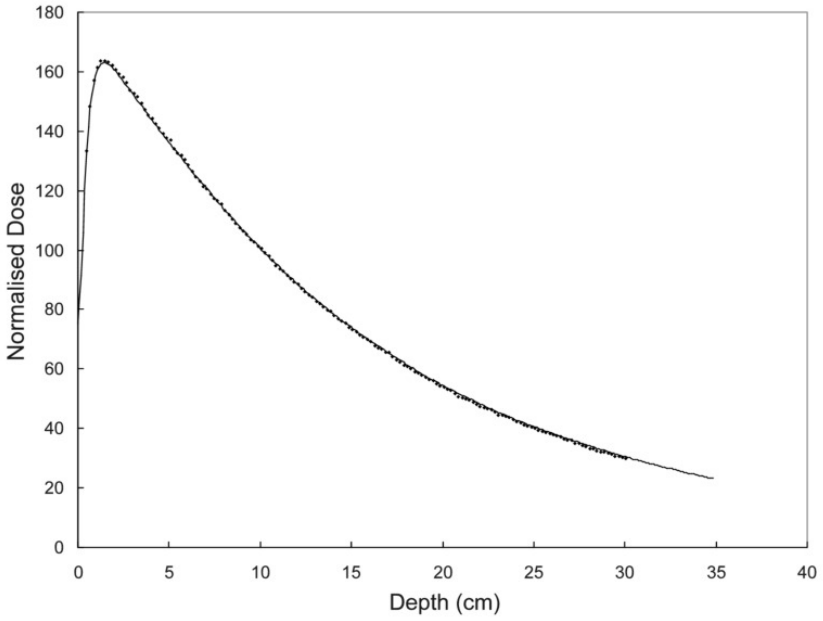

Figure 13: Depth dose curve for 4x4 cm^2 field size in water phantom. Solid line measured (CC13) and discrete points simulated. The uncertainties of the simulated values (±1SE) are represented by the size of the data points.

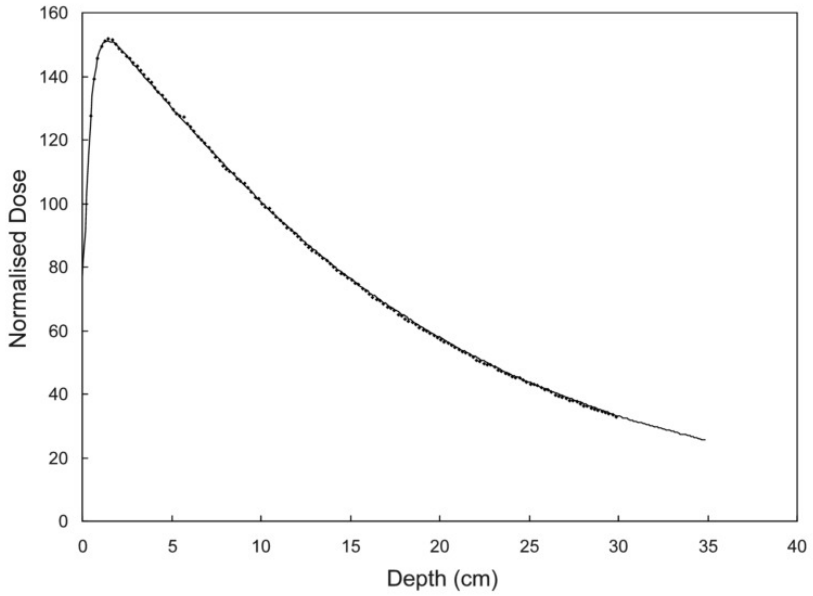

Figure 14: Depth dose curve for 10x10 cm^2 field size in water phantom. Solid line measured (CC13) and discrete points simulated. The uncertainties of the simulated values (±1SE) are represented by the size of the data points.

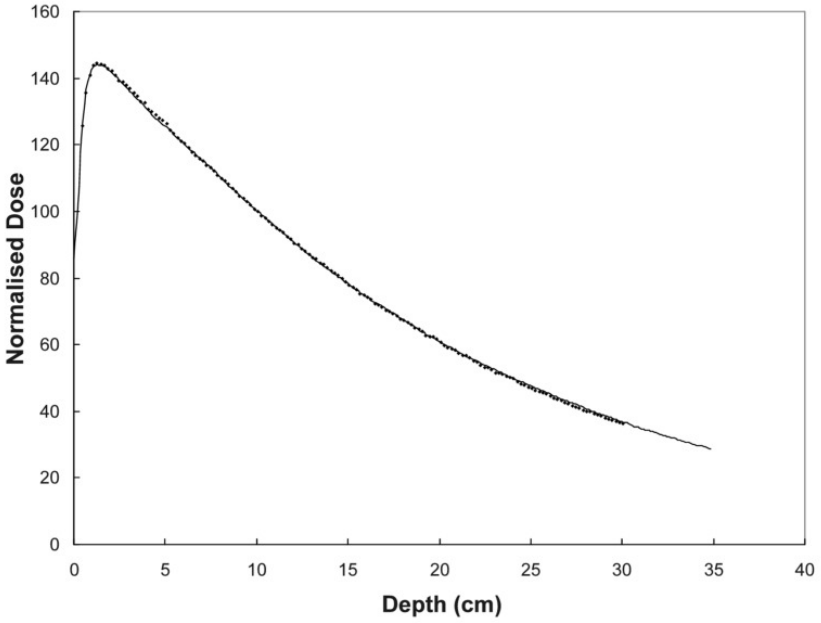

Figure 15: Depth dose curve for 20x20 cm^2 field size in water phantom. Solid line measured (CC13) and discrete points simulated. The uncertainties of the simulated values (±1SE) are represented by the size of the data points.

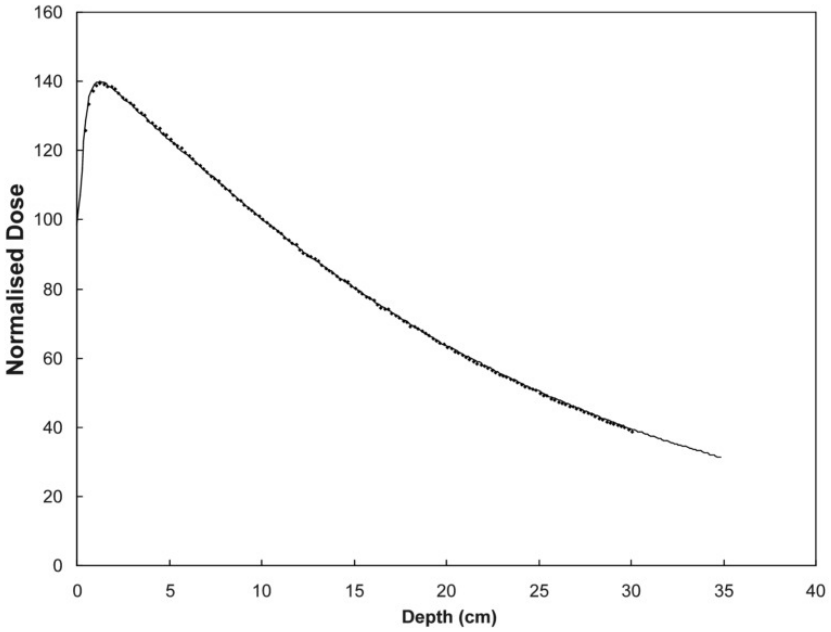

Figure 16: Depth dose curve for 40x40 cm^2 field size in water phantom. Solid line measured (CC13) and discrete points simulated. The uncertainties of the simulated values (±1SE) are represented by the size of the data points.

3.2.4 Output Factors

The result from the output-factor determination is presented in Table 3 and 4. The results from calculations based on simulated doses taken from polynomial fit of the simulated depth dose curve are presented in Table 3 and the results from calculations based on simulated doses taken from single voxels are presented in Table 4. For comparison the measured output factors are presented as well. The differences between measured and calculated values normalised to the measured value are shown in column 3. In Table 4 the uncertainty of the normalised difference between measured and simulated output factors is presented. It is seen from Table 3 that the simulated output factors do not deviate more than 2.3% from measured output factors. For field sizes smaller than 20x20 cm^2 the deviation is less than 1.65%.

Table 3: Table of results from output-factor calculations based on doses from polynomial fits of depth dose curves. First column specifies field size ratio (symmetrical fields). Column 1; measured output factors. Column 2; simulated output factors. Column 3; Difference between simulated and measured ratios in percent of the measured ratio.

	1	**2**	**3**
(cm^2/cm^2)	**Meas OF**	**Sim OF**	**[sim-meas]/meas*100**
2x2/10x10	0.79	0.80	0.16
4x4/10x10	0.86	0.87	0.93
10x10/10x10	1	1	0
20x20/10x10	1.10	1.08	-1.65
40x40/10x10	1.19	1.16	-2.30
x4y20/10x10	0.94	0.94	-0.02
x20y4/10x10	0.92	0.93	0.59

Table 4: Table of results from output-factor calculations based on doses taken from single voxels. First column specifies field size ratio (symmetrical fields). Column 1; measured output factors. Column 2; simulated output factors. Column 3; Difference between simulated and measured ratios in percent of the measured ratio. Column 4; Uncertainty (expressed as the standard error) in the quantity given in column 3.

	1	**2**	**3**	**4**
(cm^2/cm^2)	**Meas OF**	**Sim OF (voxel)**	**[sim-meas]/meas*100**	**SE of column 3**
2x2/10x10	0.79	0.79	-0.32	1.42
4x4/10x10	0.86	0.87	1.37	0.59
10x10/10x10	1	1	0	-
20x20/10x10	1.10	1.10	-0.60	0.56
40x40/10x10	1.19	1.16	-2.17	0.54
x4y20/10x10	0.94	0.94	-0.02	0.53
x20y4/10x10	0.92	0.93	0.41	0.54

3.2.5 Dose Profiles - Assymetric and Rectangular Fields

The two special cases of lateral profiles were one assymetric 10x10 cm^2 field and one rectangular 4x20 cm^2 field. The diagrams in which measured and simulated data were compared are shown in Figures 17 to 18. The assymetric field is only analysed at two depths, namely 1.5 cm and 5 cm. The assymetric field is measured in two different ways, the symmetri of the Monte Carlo model allowed for the simulated data to be mirrored and reused.

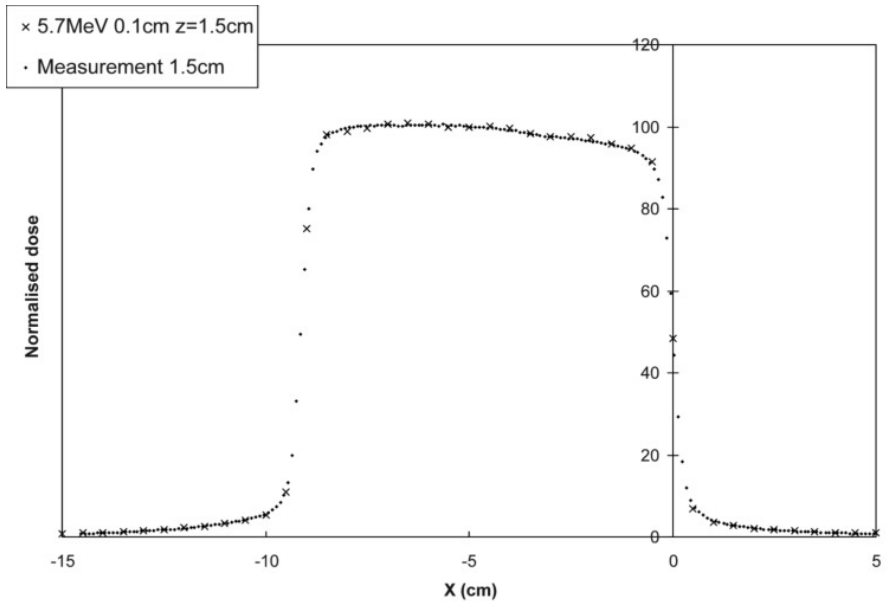
× 5.7MeV 0.1cm z=1.5cm
· Measurement 1.5cm
Normalised dose
X (cm)
120
100
80
60
40
20
0
-15
-10
-5
0
5

(a)

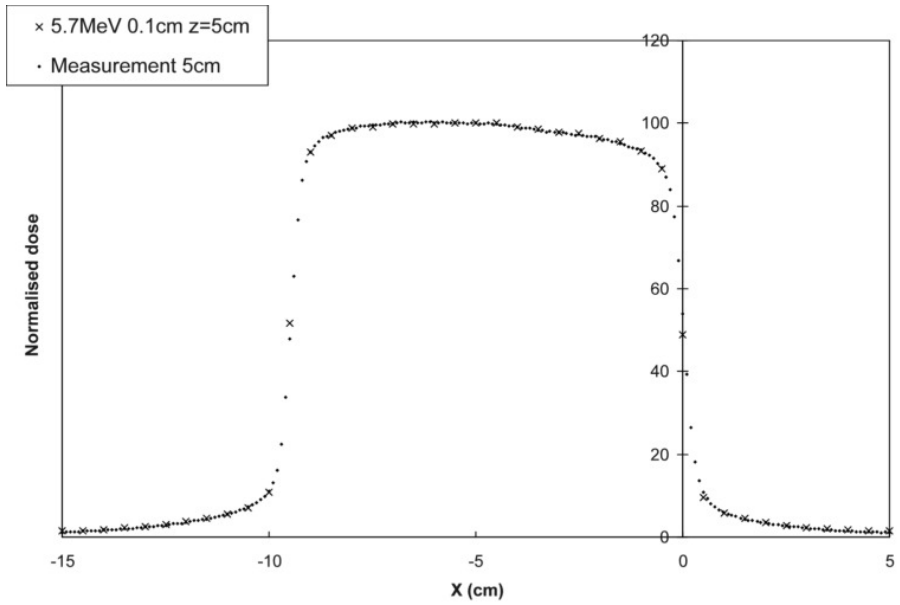
× 5.7MeV 0.1cm z=5cm
· Measurement 5cm
Normalised dose
X (cm)
120
100
80
60
40
20
0
-15
-10
-5
0
5

(b)

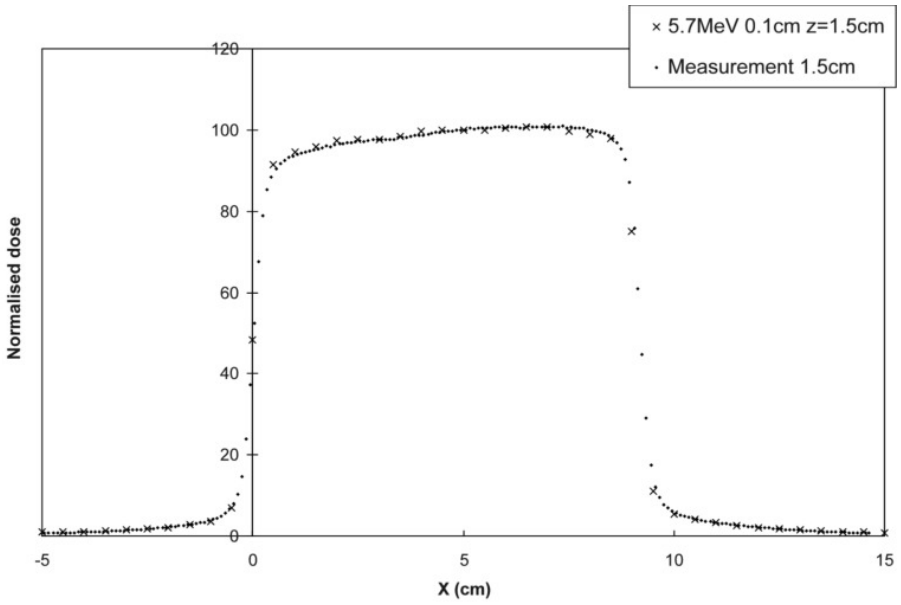

(c)

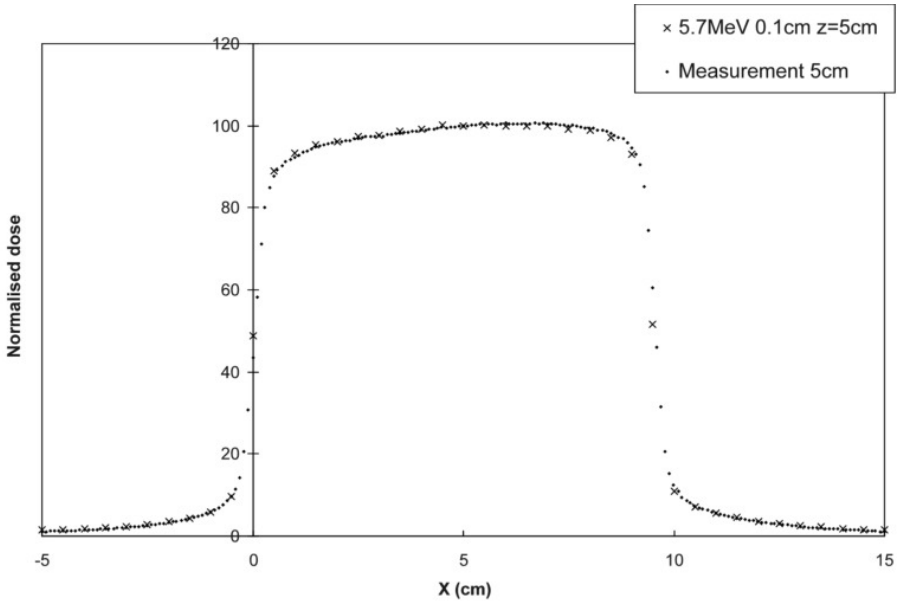

(d)

Figure 17: Dose profile for 10x10 cm^2 assymetric field in water phantom at a) 1.5 cm, b) 5 cm, c) 1.5 cm, d) 5 cm depth. Dots measured (CC04) and x simulated data. Simulated data mirrored in the dose-axis.

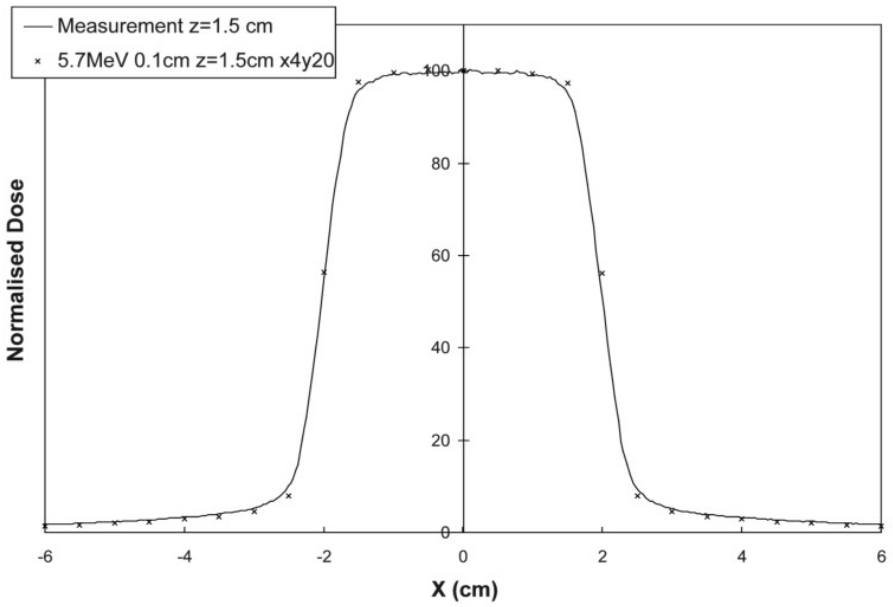
Measurement z=1.5 cm
5.7MeV 0.1cm z=1.5cm x4y20
Normalised Dose
X (cm)
0
20
40
60
80
100
-6
-4
-2
0
2
4
6

(a)

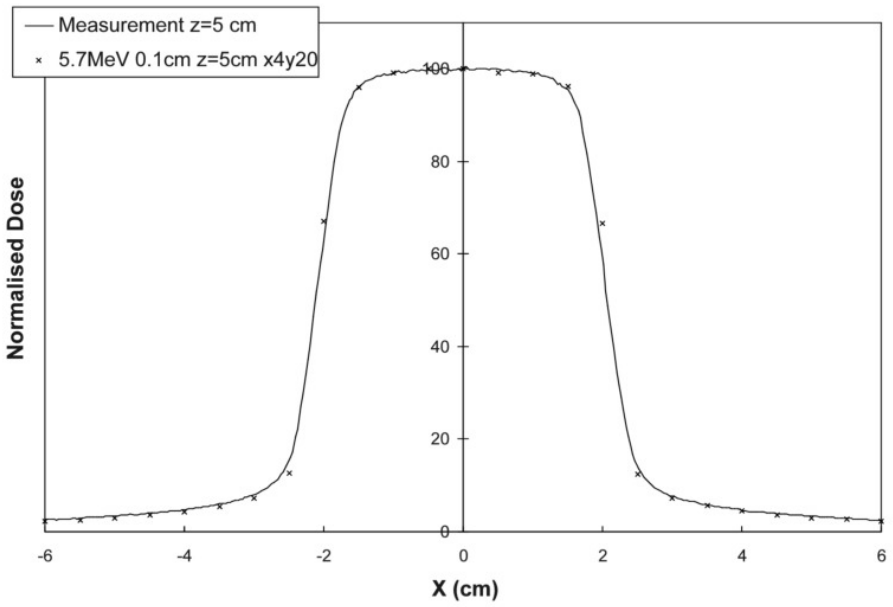
Measurement z=5 cm
5.7MeV 0.1cm z=5cm x4y20
Normalised Dose
X (cm)
0
20
40
60
80
100
-6
-4
-2
0
2
4
6

(b)

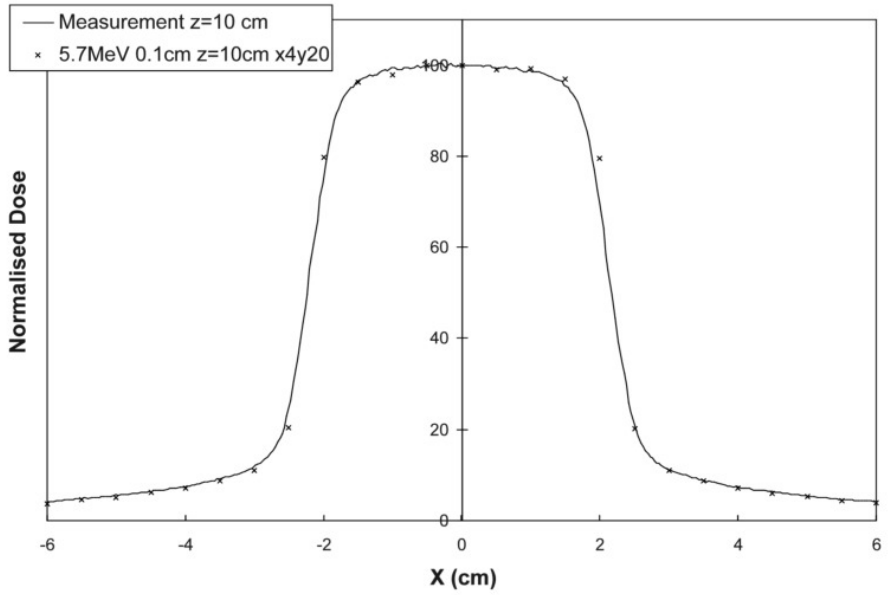

(c)

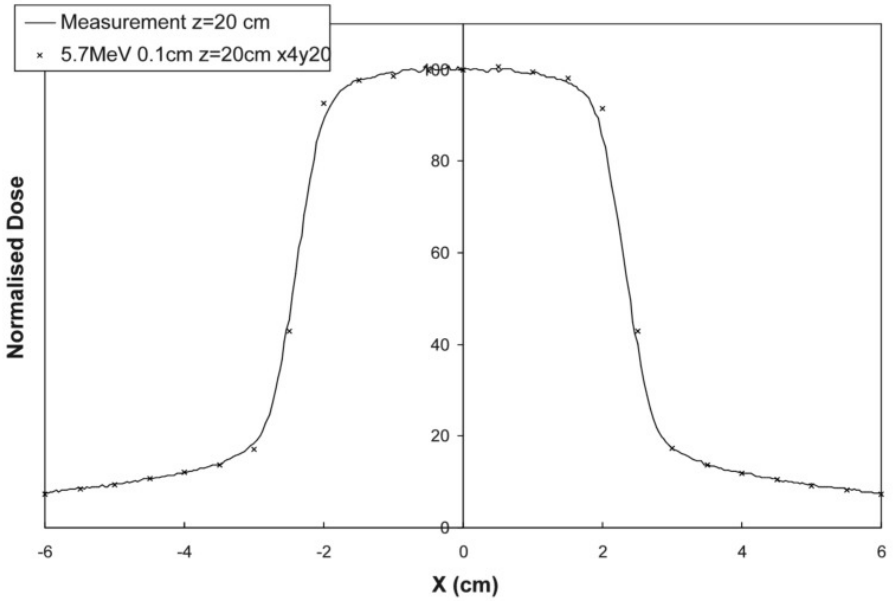

(d)

Figure 18: Dose profile for symmetric but rectangular fied 4 *cm* in the x-direction and 20 *cm* in the y-direction in water phantom at a) 1.5 cm, b) 5 cm, c) 10 cm, d) 20 cm depth. Solid line measured and discrete points (x) simulated data.

4 Concluding remarks and discussion

The optimisation of the model parameters are made with the future utilisation of the model in mind. This model is made to be used when producing DVH for determining NTCP from a dose distribution based on MC. This yields some restrictions of the model, for instance the fit of a depth-dose curve is never perfect but a compromise between dose-maximum at correct depth and good fit deeper along the curve. The model is really fitted to produce accurate dose distributions regardless of which field sizes and depths that are being used/analysed and is not fitted to produce perfect single depth dose curves or dose profiles accurate for designated depths or field sizes. If one intended to use the model for simulations of IMRT fields maybe the optimisation would have had a different approach because of the use of very small fields.

The final parameter set for modelling the Varian Clinac iX machine in room 8 at the radiation treatment department at Sahlgrenska University Hospital was chosen to be 5.7 MeV monoenergetic electrons hitting the target normally with a gaussian spatial distribution with FWHM 0.1 cm. Other authors having published results from comparable bench-marking work is; Sheikh-Bagheri & Rogers [2] who present model parameters of 5.7 MeV and 0.1 cm for a Clinac high energy machine using 3% energy spread and P. J. Keall [5] who present model parameters of 6.2 MeV and 0.13 cm FWHM for a 2100 EX Varian machine, also using 3% energy spread. B. Ask [7] presents a table of some more references and the work of adjusting modelling parameters for a Varian Clinac-23EX machine which resulted in the parameters 6.4 MeV (monoenergetic) and 0.12 cm. The result from the present work seem to stay within the variation of the results from different earlier studies.

All simulated data points in the depth dose curves deviated less than 1% of the dose at dose maximum from the measured data, except for the data points around dose max in a 2x2 cm^2 field. The criteria of maximum 1% (of the dose in dose maximum) deviation was further fullfilled in all profiles, except for those at 1.5 cm depth, where the maximum deviation was 1.7%, 1.4% and 1.5% for 10x10, 20x20 and 40x40 cm^2 field sizes respectively. The simulated output factors for fields of length smaller than 20 cm could be assessed to within 1.65% of the measured output factors.

The simulated output factors could have been more correctly assessed by doing a complete simulation of the monitor chamber. In this way the change in backscatter to the monitor chamber from the JAWS could have been accounted for. Georg X Ding [11] have done this work for a Varian CL2100EX linear accelerator. The change in dose to the monitor chamber

per incident electron hitting the target for a 6 MV beam when varying field size are in the order of the deviation between measured and simulated data in this work.

The off-axis distance in the in-air experiment was chosen to avoid a large positioning error which comes with large gradients. However it should be understood that the choice of off-axis distance did affect the resulting optimum energy from the in-air simulations. Since the results from the in-air experiment was treated only as indicative we believe the choice of off-axis distance did not influence the final parameter set.

Future work will include developing the MLC-component to be able to calculate clinical treatment plans. The developed model is also the base for analytical modelling of the accelerator head which would enable simulation of dynamic wedge.

References

[1] B. Walters D.W.O. Rogers and I. Kawrakow. Beamnrc users manual. *NRC Report PIRS-0509(A)revK*, 2009.

[2] Daryoush Sheikh-Bagheri and D.W.O Rogers. Sensitivity of megavoltage photon beam monte carlo simulations to electron beam and other parameters. *Med. Phys.*, 29, 379-390 (2002).

[3] K. Aljarrah *et. al.* Determination of the initial beam parameters in monte carlo linac simulation. *Med. Phys.*, 33, 2006.

[4] J Pena et. al. Comissioning of a medical accelerator photon beam monte carlo simulation using wide-field profiles. *Phys. Med. Biol.*, 49:4929–4942, 2004.

[5] P. J. Keall et. al. Determining the incident electron fluence for monte carlo-based photon treatment planning using a standard measured data set. *Med. Phys.*, 30, 2003.

[6] E. Sham *et. al.* Influence of focal spot width on characteristics of very small diameter radiosurgical beams. *Med. Phys.*, 35, 2008.

[7] B. Jutemark. Monte carlo based investigation of the influence of accelerator-head geometry on megavolt photon beam quality in radiotherapy. *Masters thesis, Lund University*, LUJI-RADFY-EX-1/2005, 2005.

[8] F. Hasenbalg et. al. Vmc++ versus beamnrc: A comparison of simulated linear accelerator heads for photon beams. *Med. Phys.*, 35, 1521-1531 (2008).

[9] J. H. Hubbell and S. M. Seltzer. Tables of x-ray mass attenuation coefficients and mass energy-absorption coefficients 1 kev to 20 mev for elements z=1 to 92 and 48 additional substances of dosimetric interest. *Technical Report NISTIR 5632*, NIST, Gaithersburg, MD, 1995.

[10] B. R. B. Walters *et. al.* History by history statistical estimators in the beam code system. *Med. Phys.*, 29, 2745-2752 (2002).

[11] George X Ding. Using monte carlo simulations to comission photon beam output factors - a feasibility study. *Phys. Med. Biol.*, 48, 2003.

APPENDIX

Depth dose simulations - build-up region

Depth doses have been simulated in two different ways (A and B). A) with the module CHAMBER in BEAMnrc using version released 2005. B) with DOSXYZ using version released 2009 and file format .IAEAphsp . Simulations with the CHAMBER module in beam were first made with poor resolution in the build-up region and then a simulation with 1mm resolution between 0.1 and 2 cm depth. The results of method A and B are compared in Figure 19 and 20. The DOSXYZ-simulations are made in 1 cm^2 square pixels and the CHAMBER simulations are made in standing cylinders with 0.75 cm radius and 0.5 cm height.

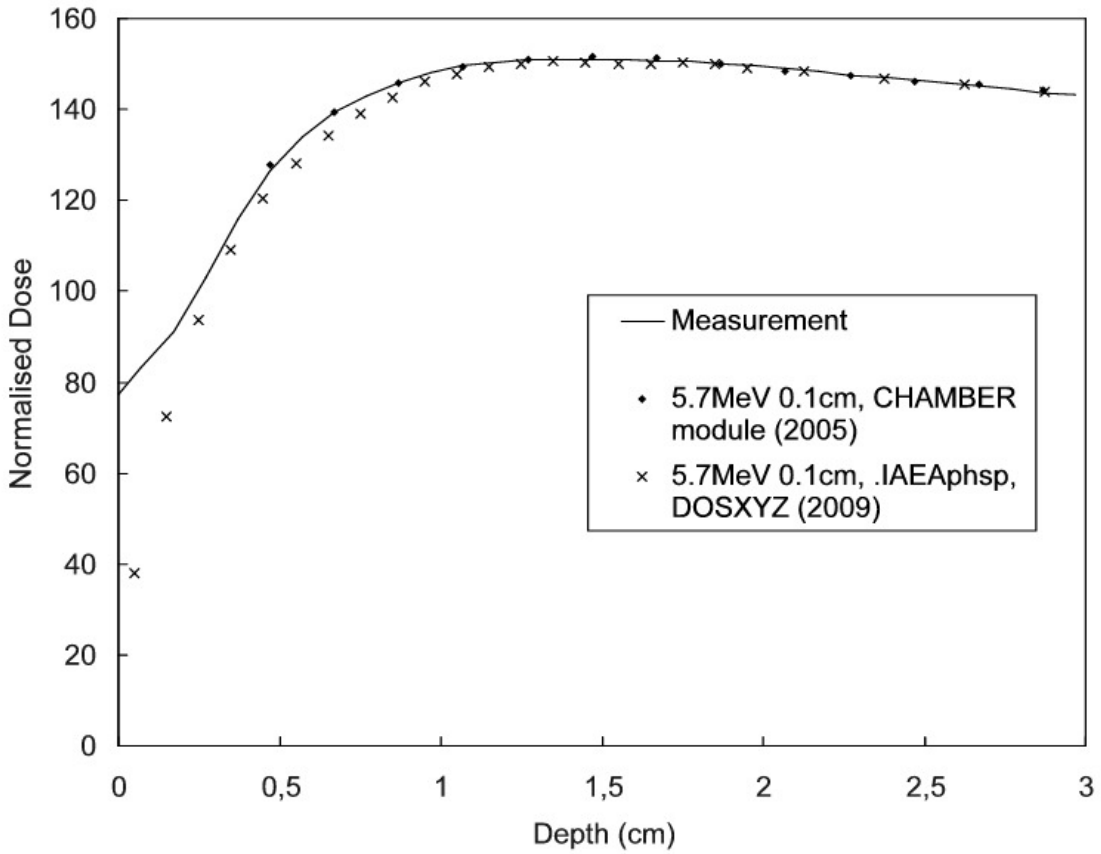

Figure 19: Simulation made with BEAMnrc module CHAMBER with poor resolution in the build-up region compared to simulation made with DOSXYZ (x). Difference is seen at shallow depths. Solid line shows measured depth dose (CC13).

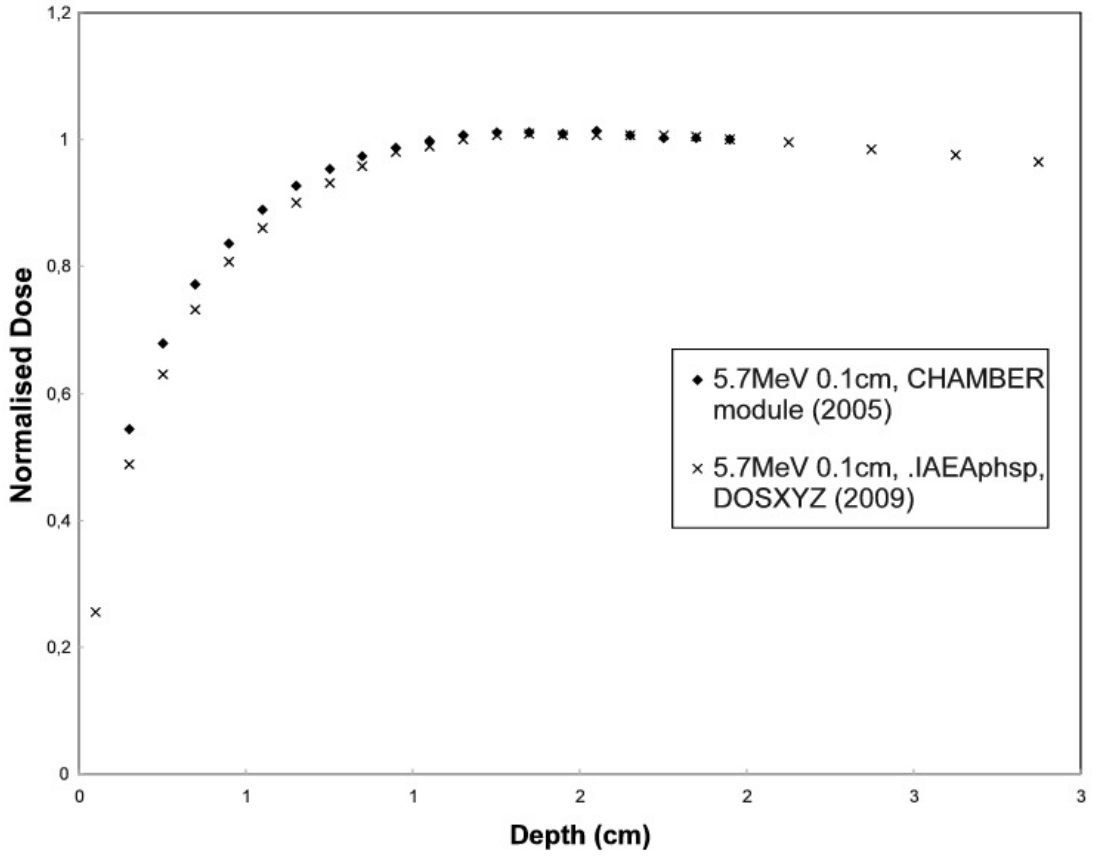

Figure 20: Simulation with CHAMBER module with 1 mm resolution in the region 0.1-2cm depth compared to simulation with DOSXYZ (x - same curve as in Figure 19).Differences is again seen at shallow depths.

Beyond dose maximum the two methods/versions overlap. More literature study has to be made to understand the differences in versions and method and to understand which one is most correct.

Excerpt of list files

On the following two pages an example of list-file is shown from the accelerator head simulations in BEAMnrc, it has been cut before the detailed description of accelerator head is given.

```
 NRCC CALN: BEAMnrc(EGSnrc) Vnrc(Rev 1.78 of 2004-01-12 11:44:06-05),
(USER_MACROS Rev 1.5)
 ON i686-pc-1-gnu                                          15:09:20 Sep 25 2009
 ****************************************************************************
 **                                                                        **
 **                                BEAMnrc                                 **
 **                                                                        **
 **      Code developed at National Research Council of Canada as part of  **
 **           OMEGA collaboration with the University of Wisconsin.        **
 **                                                                        **
** This is version V1 of BEAMnrc (Rev 1.78 last edited 2004-01-12 11:44:06-05**
 **                                                                        **
 ****************************************************************************


 Max # of histories: to run    10000000          To analyze         10000000
                   Incident charge                                    -1
                   Incident kinetic energy                 5.700 MeV

                   Bremsstrahlung splitting                DIRECTIONAL
                    splitting field radius                   20.000 cm
                    splitting field SSD                     100.000 cm
                    splitting no. in field                       1000
                    e+/e- will be split at plane  20 in CM   3:
                     Z of splitting plane                    12.500 cm
                     Z of Russian Roulette plane             12.300 cm
                     Radial redistribution of split e+/e-  ON
                   Photon force interaction switch         OFF
                   SCORING PLANES:     #           CM #
                   --------------------           ----
                                       1             7
                   Phase space files will be output at EVERY scoring plane
                   Range rejection switch                  ON
                   Range rejection in  61 regions
                   Automatic ECUTRR used starting from          0.700 MeV
 Range rejection based on medium of region particle is traversing
 Maximum electron ranges for restricted stopping powers:
   kinetic            Range for media 1 through 5
   energy                          (g/cm**2)
   (MeV)    AIR700IC  W700ICRU  CU700ICR  W700ICRU  KAPTON70
   0.200       6.072     0.002     0.002     0.002     0.005
   0.400      84.941     0.010     0.016     0.011     0.070
   0.600     178.342     0.020     0.033     0.021     0.146
   1.000     383.457     0.041     0.069     0.043     0.317
   1.500     651.119     0.069     0.118     0.072     0.543
   2.000     921.052     0.097     0.167     0.101     0.775
   4.000    1984.479     0.208     0.362     0.217     1.714
   5.700    2862.394     0.301     0.527     0.314     2.511
                   Discard all electrons below K.E.:         2.000 MeV
                        if too far from closest boundary
                   Maximum cputime allowed                   900.00 (hrs)
                   Initial random number seeds             25            30
           LATCH_OPTION = 2: Latch values inherited, origin of
                             secondary particles recorded.

==============================================================================

                   Electron/Photon transport parameter

==============================================================================

 Photon cross sections                                      PEGS4
 Photon transport cutoff(MeV)                               AP(medium)
 Pair angular sampling                                      KM
 Pair cross sections                                        BH
```

Triplet production	Off
Bound Compton scattering	ON
Radiative Compton corrections	Off
Rayleigh scattering	OFF
Atomic relaxations	OFF
Photoelectron angular sampling	ON
Electron transport cutoff(MeV)	AE(medium)
Bremsstrahlung cross sections	NIST
Bremsstrahlung angular sampling	KM
Spin effects	On
Electron Impact Ionization	OFF
Maxium electron step in cm (SMAX)	0.1000E+11
Maximum fractional energy loss/step (ESTEPE)	0.2500
Maximum 1st elastic moment/step (XIMAX)	0.5000
Boundary crossing algorithm	EXACT
Skin-depth for boundary crossing (MFP)	3.000
Electron-step algorithm	PRESTA-II

==========

Material summary 5 Materials used

#	Material	density(g/cm**3)	AE(MeV)	AP(MeV)	UE(MeV)	UP(MeV)
1	AIR700ICRU	1.205E-03	0.700	0.010	55.511	55.000
2	W700ICRU	1.930E+01	0.700	0.010	55.511	55.000
3	CU700ICRU	8.933E+00	0.700	0.010	55.511	55.000
4	W700ICRU18	1.800E+01	0.700	0.010	55.511	55.000
5	KAPTON700ICRU	1.420E+00	0.700	0.010	55.511	55.000

SOURCE PARAMETERS

INITIAL PARTICLES are Electrons
PARALLEL BEAM WITH 2-D GAUSSIAN X-Y DISTRIBUTION
ON FRONT FACE at Z= 0.0000 cm
BEAM SIGMA= 0.0425 cm (FWHM= 0.1000 cm)
X,Y,Z DIRECTION COSINES = (0.00000 0.00000 1.00000)

KINETIC ENERGY OF SOURCE = 5.700 MeV

Modification made in beamDP